EXPERIMENTAL VERIFICATION OF AN ORIENTATION ESTIMATION TECHNIQUE FOR AUTONOMOUS ROBOTIC PLATFORMS

By

IYAD F.I. HASHLAMON

Submitted to the Graduate School of Engineering and Natural Science in partial fulfillment of the requirements for the degree of
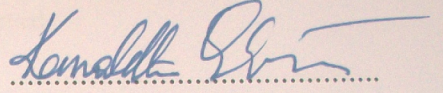
Master of Science

Sabanci University

January 2010

EXPERIMENTAL VERIFICATION OF AN ORIENTATION ESTIMATION TECHNIQUE FOR AUTONOMOUS ROBOTIC PLATFORMS
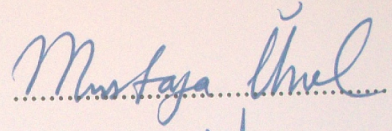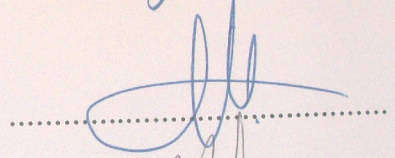
IYAD F.I. HASHLAMON

APPROVED BY:

Assist. Prof. Dr. Kemalettin Erbatur
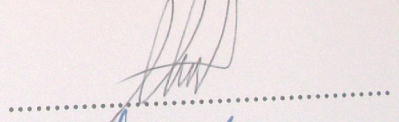(Thesis Supervisor)

Assoc. Prof. Dr. Mustafa Ünel

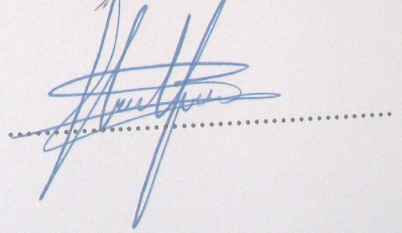Assoc. Prof. Dr. Mahmut Akşit

Assist. Prof. Dr. Ahmet Onat

Assist. Prof. Dr. Hüsnü Yenigün

DATE OF APPOVAL......19/01/2010...............

أهديها لأبي، أمي،أخواني، أخواتي، وخطيبتي

To my Parents, Brothers, Sisters, and Fiancé

ACKNOWLEDGMENTS

EXPERIMENTAL VERIFICATION OF AN ORIENTATION ESTIMATION TECHNIQUE FOR AUTONOMOUS ROBOTIC PLATFORMS

Iyad F.I. Hashlamon

ME Master's Thesis, 2010

Thesis Supervisor Assist. Prof. Dr. Kemalettin ERBATUR

Abstract

Research on autonomous platforms ranging from unmanned aerial and underwater vehicles to wheeled, tracked and legged machines enlarges the application boundaries of robotic systems. The control of these platforms, however, is a challenging task which requires the availability or estimation of various feedback variables. Orientation information of the autonomous platform is vital for robotic control.

A variety of approaches and instruments are reported in the literature for orientation estimation with inertial sensors. Many approaches are based on Kalman filters. The use of Extended Kalman filters (EKF), Unscented Kalman filters and complimentary Kalman filters are proposed too.

This thesis concentrates on the estimation of orientation from measurements provided by inertial sensors. The use of three-axial linear accelerometers and rate gyros is considered. The sequential use of two estimators is proposed for orientation estimation. The first one is a Kalman Filter and it is employed for the gravity estimation mainly based on acceleration readings. The second estimator has the structure of an Extended Kalman Filter which uses the gravity estimate generated by the first estimator and rate gyro readings for the orientation estimation. Orientation is estimated in a multivariable fashion, without the simplifying assumption of decoupling between one-dimensional rotations about the three gyroscope axes. Therefore quite large angles of rotation can be handled accurately.

The presented approach uses a quaternion representation which avoids representation singularities common with orientation descriptors like Euler angles. The computational efficiency is improved by the quaternion representation too.

In order to test the estimation methods, experimental studies are carried out. A three-degrees-of-freedom robot is designed and built. The accelerometer and gyroscope unit is mounted at the tool end of this manipulator which generated test motion in the experiments. In order to create a basis for comparison, robot joint encoder data is used and actual rotation matrices during the motion are computed. The experiments indicate that the proposed technique delivers reliable orientation estimates in a large range of rotation angles and motion frequencies.

BİR OTONOM ROBOT YÖNELİM TAHMİN TEKNİĞİNİN DENEYSEL DOĞRULANMASI

Iyad F.I. Hashlamon

ME Yüksek Lisans Tezi, 2010

Tez Danışmanı Y. Doç. Dr. Kemalettin ERBATUR

Özet

İnsansız hava araçlarından deniz altı araçlara ve tekerlekli, paletli, bacaklı makinalara varan konularda yürütülen araştırmalar robot sistemlerinin uygulama alanlarını genişletmektedirler. Ne var ki, bu tür platformların kontrolü geri beslemede kullanılan birçok değişkenin tahmin edilmesini gerektiren zor bir görevdir. Otonom platformun yönelim bilgisi robot kontrolü için hayati önem taşır.

Literatürde atalet sensörleri ile yönelim tahmini için çeşitli yaklaşım ve enstrümanlar rapor edilmiştir. Birçok yaklaşım Kalman süzgeçlerine dayalıdır. Genişletilmiş Kalman süzgeçlerinin (EKF), Kokusuz Kalman süzgeçlerinin ve tümleştirici Kalman süzgeçlerinin kullanımı da önerilmiştir.

Bu tez atalet sensörlerinin sağladığı ölçümlere dayanan yönelim tahmini üzerinde yoğunlaşmaktadır. Üç eksenli doğrusal ivmeölçerlerin ve jiroskopların kullanımı üzerinde durulmaktadır. Yönelim tahmini için iki tahmin algoritmasının ardışık kullanımı önerilmektedir. Bunlardan ilki bir Kalman süzgecidir ve bu süzgeç ana olarak ivmeölçer verilerine dayanan bir yer çekimi tahmini için kullanılmaktadır. İkinci algoritma Genişletilmiş Kalman filtresi yapısındadır ve ilk algoritma ile elde edilen yer çekimi tahminini ve jiroskop verilerini kullanarak yönelim tahminini gerçekleştirmektedir. Yönelim, jiroskop eksenleri çevresindeki tek boyutlu dönüşlerin ayrıklığı basitleştirici varsayımı kullanılmaksızın, çok değişkenli bir şekilde tahmin edilmektedir. Bu şekilde, oldukça büyük dönüş açıları hassas bir şekilde ele alınabilmektedir.

Sunulan yaklaşım bir kuaterniyon gösterimini kullanmaktadır. Bu gösterim Euler açıları gibi bir takım gösterimlerde rastlanan gösterim singülaritelerini engellemektedir. Kuaterniyon gösterimi ile algoritmanın bilgisayarda işlenme yükü de azalmaktadır.

Tahmin yöntemlerini teste tabi tutmak için deneysel çalışmalar yapılmıştır. Üç serbestlik dereceli bir robot tasarlanmış be imal edilmiştir. İvmeölçer ve jiroskop birimi deneylerde test hareketlerini gerçekleştiren bu manipülatörün uç platformuna monte edilmişlerdir. Karşılaştırmaya baz teşkil etmesi için robot enkoderlerinden okunan eklem konumları hareket sırasında gerçek dönüş matrislerinin hesaplanmasında kullanılmışlardır. Deneyler, önerilen tekniğin geniş dönüş açısı ve hareket frekansı aralıklarında güvenilir yönelim tahminleri ürettiğini göstermektedir.

TABLE OF CONTENTS

LIST OF FIGURES

LIST OF TABLES

1   INTRODUCTION

The orientation estimation of a platform is the estimation of its body attitude in 3-D with respect to a reference frame using sensors data. In this thesis the reference frame is a world fixed coordinate system and the estimation uses measurements from a 3-axes accelerometer and a 3-axes rate gyroscope.

The determination of orientation of an autonomous robotic platform from imperfect data plays an important role in the control. The estimated body attitude is used in the control loops of these systems. The success of estimation depends on several factors. The main factor can be listed as: i) Quality of sensors (such as inertial measurement units, gyroscopes, accelerometers, magnetometers and GPS based measurement systems), ii) Estimation method implemented (such as observers and Kalman filters), iii) Orientation representation employed (such as rotation matrices, Euler angles, fixed axes rotation angles and quaternions).

Although in certain applications a high quality gyroscope can be used for the attitude calculation by integration alone, such precise gyroscopes are expensive. Relatively more affordable gyroscopes have bias and noise problems and produce generally unsatisfactory results by integration alone. The accelerometer can be used for the orientation estimation too. However, it functions satisfactorily only for low frequency ranges. Therefore, providing a cost-effective solution under adverse effects of noise and sensor bandwidth limitations is a challenge calling for sophisticated estimation techniques.

Kalman filtering presents a strong solution. It combines the strengths of observers and Bayesian approaches. In a Kalman filter, predicted data are compared with measured data and their difference is fed back to the system over a state estimation correction gain. This gain is determined in a statistically optimal way and noise

characteristics (probability distributions associated with the process and sensor noise signals) are used in its computation, unlike deterministic observer gains. For plants with nonlinear state space descriptions, a modification of the Kalman Filter, an Extended Kalman Filter (EKF) can be employed. Although the optimality of the state estimation correction gain is compromised, quite satisfactory estimation performance can be obtained by the EKF.

A considerably great effort has been done in the fusion of the inertial sensing instruments using Kalman filters in many perspectives such as navigation, aircraft technology, and biomechanics. Fusion methods have dramatically gained an increased interest. In reported studies on orientation estimation with accelerometer and rate gyroscope sensor data, Kalman filtering is used in such a way to solve the trade-off between a good short-term precision (when a gyroscope is used) and a reliable long-term precision (when accelerometer is used). A combination of the measurements of the two instruments in order to make use of the advantages of each instrument and alleviating their limitations is sought. However, most methods have their limitations, such as the assumption of well known gravity, working for low angles, singularities, high computational cost, and no guarantee for error bound.

The estimation scheme also depends on the orientation representation employed. Roll-Pitch-Yaw angles, Euler angles, rotation matrices, axis-angle representations, and unit quaternions are commonly used representations of orientation. Each of these has its own advantages and disadvantages. The Euler angle representation is simple but has high computational cost and singularities. Rotation matrices are easy to use with no singularities and moderate computational cost. The quaternion representation has no singularities too and it presents the lowest computational cost although but it has no direct physical interpretation.

The next section presents a literature survey on the use of sensors, attitude representations and techniques employed for orientation estimation.

1.1   A Survey on Orientation Estimation

The rapid and high technological development in inertial measurement units (IMU) makes them popular and widely used. Amongst commonly used instruments are, gyroscopes, accelerometers, and magnetometers.

The attitude estimation can be realized using a combination mechanism of the above mentioned sensors. The integration of the instantaneous angular velocity measured by a very high quality gyroscope can be used for the attitude estimation of dynamic systems [1]. However, these gyroscopes have to be accurate and produce a stable output which makes them very expensive. At the same time; the ordinary gyroscopes have bias and noise which limit their estimation capability to short time running [2]. The accelerometers are contaminated by the sensor noise which limits their estimation to work in the low frequency region, and they measure both linear and gravity accelerations. The magnetometers are disturbed by metals [3]. Combining accelerometers and magnetometers is another way for attitude estimation [4], where the deduced gravity from the accelerometer signal used to estimate the roll and pitch angles while the yaw angle is estimated from both signals. Although [4] presents a simple method, the accelerometer signal used has components other than the gravity acceleration and these components affect the estimated results.

Some of the studies used the gyroscope with GPS, others used GPS with magnetometers and accelerometers, or used gyroscope, magnetometers and accelerometers together [5-7].

The attitude estimation for a flying vehicle [8] from a low-cost IMU and 3-axis magnetometer measurements using two nonlinear complementary filters is done with the Euler angles representation. However, this study is realized only for the mentioned system in takeoff and landing. A linear complementary filter is used in [9] for roll and pitch angle estimation by fusing the measurements from the gyroscopes and the tilt-meters in the frequency domain, assuming small variations of orientation angles. In [10] an estimated virtual angular velocity provided by the low pass sensors is used for the bias estimate and the complimentary filter is used afterwards to recover the actual attitude.

Kalman filter [11] is helpful for the orientation estimation in combining the data from several noisy measurements. That is because it incorporates the observer theory and the Bayesian approach [12]. Kalman filters are like observer models. As a result, they can be used for modeling complex, dynamic and continuous systems. However, the gain determination depends on the noise or the probability distribution associated with the sensor signals unlike the deterministic gain of the observer.

The Kalman filter used in [13] uses 3-axes accelerometers, 3-axes gyroscopes and magnetometers for attitude estimation. The method uses the Euler angles representation and it assumes the availability of the estimated linear acceleration. This assumption does not hold in all cases and the Euler representation has the disadvantage of representation singularities too. A Kalman filter and an Extended Kalman filter with quaternion representation were used for the estimation using the Newton method or Gauss-Newton method to find a corresponding quaternion for each pair of accelerometer and magnetometer measurements [14, 15]. The computed quaternion is then combined with the angular rate measurements, and presented to the Kalman filter as its measurement. In the same context, instead of using Gauss-Newton method, the quaternion estimator algorithm [16, 17] is used in [18] to calculate the attitude of the system with respect to a fixed frame. [18] computes the quaternion which rotates the measured vectors to the fixed frame. For better performance, the Factored quaternion algorithm [19] is used for the same purpose in [18]. It estimates the orientation based on measurements of three sequential rotations about three orthogonal axes.

In [20], a switching algorithm with a Kalman filter is used to switch between high and low acceleration cases for a walking robot, for the attitude estimation using a gyroscope (assuming exact angular velocity measurements) and an accelerometer. In this study, the bias is not considered during the derivation. In low acceleration the linear acceleration is assumed to be zero and hence the accelerometer reading is the gravity vector whereas in high acceleration the linear acceleration is treated as an unknown disturbance.

Other reports used Kalman filter with strapdown integration. Strapdown with quaternion representation approach was studied in [21] where the gyroscope is used when the body is in motion while the accelerometer is used in the static inclination by double integrating the acceleration. However, this work is only applicable to periodic

4

movements. In [22] the strapdown integration is used to find a predicted orientation estimate, and this estimate is then corrected by two methods: The first one considers the accelerometer reading as gravity vector which corrects the predicted quaternion. The second method uses corrected quaternion samples to form a linear interpolation between them, and then corrects the other samples in between the two corrected samples. A quaternion Kalman filter is introduced in [23] where the quaternion is corrected depending on the linear pseudo measurement equation of gravity. The quaternion constrained Kalman filter is used in [24] which keeps the unity norm of the quaternion.

An accelerometer with a magnetometer for low frequency components, and the gyroscope for high frequencies were utilized to track the human limbs in real time in [25]. Nevertheless, this study is applicable to 2D, and magnetometers have a problem in the vicinity of ferromagnetic metals. Similarly, inclination using both gyroscope and accelerometer is estimated and then the difference between them is used in complementary Kalman filter for the final estimation in [26]. However, it operates on the errors of the primary estimated states with no guarantee on the bound of this error especially for long time operations [27].

The Extended Kalman filter is widely used for the estimation of nonlinear system behavior [28]. The EKF is employed with several fusion approaches and orientation representations. EKF applications with quaternion representation can be found in [29, 30, 32], and EKF with Euler representation is reported in [31]. Its principle is finding the Jacobian for both the process function and the measurement function forming a state space representation linearized around the estimated state. However, Jacobian matrices may be difficult to be obtained for high order systems. Furthermore, the linear approximation of the system may introduce errors in the state which may lead the state to diverge over time [33].

In [34] the EKF with Euler representation is used to estimate the roll and pitch angles. It considers an inclinometer when the acceleration is lower than a threshold whereas it only integrates the gyroscope reading when the acceleration is higher than the threshold. In [35], EKF is used for the real time attitude estimation of a spacecraft using the quaternion representation:

The unscented Kalman filter (UKF) is used for nonlinear system without linearization. It works by using the same nonlinear function to propagate a fixed number of sigma points [33, 36]. For a comparison with the EKF, the UKF is used in [37] with quaternion representation to estimate the attitude of a spacecraft. Better results are obtained with the UKF. However, the knowledge of the system function is necessary for the application of this filter.

1.2   Overview of the Thesis

As mentioned above, in this study, a 3-axes accelerometer and 3-axes gyroscope are used for full orientation estimation (Figure 1-1).

The accelerometer output consists of the gravity acceleration, linear acceleration, bias and noise. The gravity acceleration vector as expressed in the robotic platform (body) frame contains information about the roll and pitch angles of the body. To extract the gravity acceleration, the accelerometer output signal has to be decomposed. First of all, the linear acceleration component in the accelerometer output is modeled as slow (low pass filtered) version of the actual linear acceleration. By ignoring the noise, the values of the accelerometer signal terms are predicted using a pseudo inverse matrix multiplication. The predicted values are used as initial values for an accelerometer Kalman filter which updates the predicted terms and corrects them. An z-y-x-Euler angles representation is employed for orientation. The gravity acceleration estimate is used for the computation of x- and y-Euler angles.

The accelerometer Kalman filter described above can function as a orientation estimator by its own, especially for low frequencies of motion. However, much better estimates can be obtained when its output is combined with gyroscope based estimates.

In the proposed approach, the accelerometer Kalman filter works sequentially with an Extended Kalman filter which processes the angular rate measurement of the gyroscope and produces a unit quaternion estimate for the orientation description of the body. The z-y-x- Euler angles estimated by the accelerometer Kalman filter are transformed into quaternion representation to be considered as a "measured quaternion"

6

for the correction stage of the gyroscope Extended Kalman filter. Since in addition to the x- and y- Euler angles obtained from the gravity estimate, the z-Euler angle is also required to compute the measured quaternion, the accelerometer Kalman filter "borrows" this angle from the quaternion estimate of the gyroscope Extended Kalman filter.

In other words, the two filters feed each other cyclically: The gyroscope filter provides the z-Euler angle for the accelerometer filter, whereas the accelerometer filter produces the measured quaternion for the gyroscope filter. Figure 1-2 illustrates the sequential operation of the two filters.

The working principle of the gyroscope Extended Kalman filter can be outlined as follows. A state space model which relates the unit quaternion evolution with the measured angular velocity, gyroscope bias and noise is obtained. This model is a nonlinear one. It is used in the quaternion prediction. The prediction is corrected by the use of the accelerometer filter output as the measured quaternion. This correction is followed by a norm correction to keep the unity magnitude of the quaternion.

The performance of the estimation system is tested by experiments with a robotic platform. This platform has a fixed base and joint encoder readings provide a means of computing the actual orientation. Experimental results indicate that the proposed estimation technique provides stable and reliable orientation estimates for a large range of orientation angles and motion frequencies.
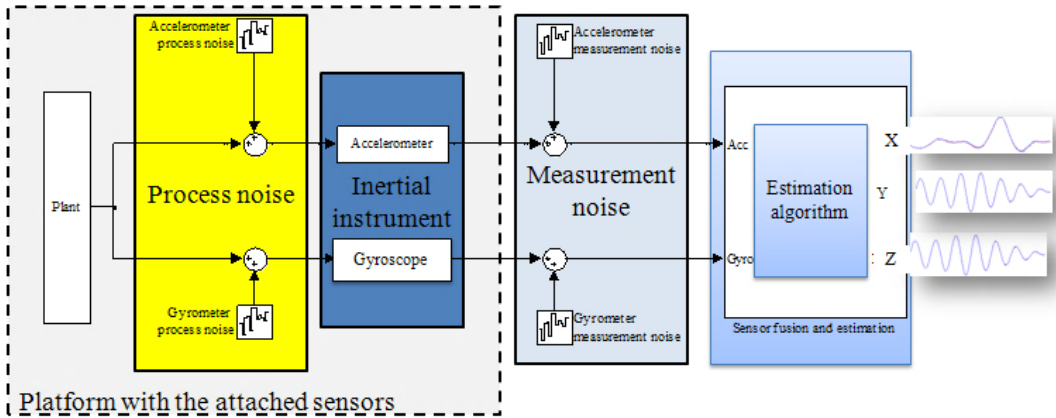
Figure 1-1: Signal flow schematic diagram
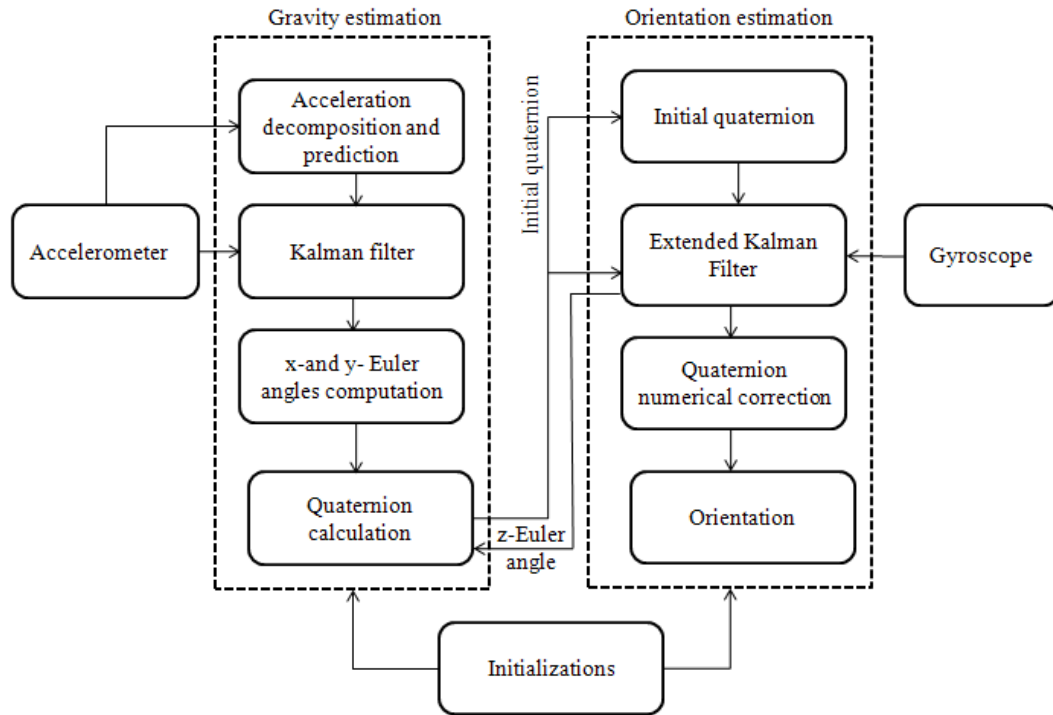
Figure 1-2: Estimation block diagram

1.3 Contribution

The main contributions of this thesis are:

- Full decomposition of the accelerometer signal terms, and estimation of the gravity vector which can be used for the orientation estimation for low frequencies.
- The estimation algorithm which produces stable and reliable estimates with the sequential use of a Kalman filter and an Extended Kalman filter.

1.4   Thesis Organization

This thesis is organized as follows. In Chapter 2, preliminary concepts are introduced. Accelerometer and gyroscope model equations employed in this thesis, attitude representations, basic quaternion mathematics, Kalman and Extended Kalman filter equations are reviewed. In Chapter 3, the decomposition of the accelerometer signal and the estimation of the gravity vector based on accelerometer data are presented. The Extended Kalman filter based orientation estimator with unit quaternion representation is described in Chapter 4. Chapter 5 is devoted to the experimental results. The conclusion is presented in the last chapter.

2   PRELIMINARIES

Basic models of the sensors, attitude representations and Kalman filter equations are reviewed in this chapter.

2.1   Accelerometer Model

Accelerometers measure the acceleration of a moving body depending on the Hooke's law and Newton's second law of motion [38].

The general output of the accelerometer is given [39] in the form

$$y_{Ak} = a_{fk} - g_{Ak} + b_{Ak} + v_{Ak} \tag{2.1}$$

$$b_{Ak} = b_{Ak-1} + v_{bAk-1} \tag{2.2}$$

where k is the sampling index. y_{Ak} stands for the accelerometer output and b_{Ak} is a bias term. v_{Ak} and v_{bAk} represent the sensor and bias noise terms, respectively. They are assumed to be independent random variables with zero mean Gaussian distribution functions and variances $\sigma_{b_A}^2, \sigma_{v_A}^2$ respectively. g_{Ak} is the gravity acceleration. (It is typically $[0 \ 0 \ 9.81]^T$, as expressed in a coordinate frame with its z-axis showing downwards to the earth's surface.). a_{fk} is a "slower" version of the linear acceleration a_k. In this thesis, the relation between a_{fk} and a_k for each acceleration axis of the accelerometer is modeled by a first-order low pass filter:

$$\frac{a_{f_x}(s)}{a_x(s)} = \frac{k_p}{\tau s + 1}, \qquad \frac{a_{f_y}(s)}{a_y(s)} = \frac{k_p}{\tau s + 1}, \qquad \frac{a_{f_z}(s)}{a_z(s)} = \frac{k_p}{\tau s + 1} \qquad (2.3)$$

Gain K_p and the time constant τ are case-specific design parameters. With a rearrangement of (2.3) we obtain

$$\tau a_f(s)s + a_f(s) = k_p a(s), \qquad (2.4)$$

which, by the inverse Laplace transform, yields

$$\tau \dot{a}_f(t) + a_f(t) = k_p a(t). \qquad (2.5)$$

The backward Euler rule is used to obtain a discrete time approximate of this differential equation as

$$\tau \frac{a_{fk} - a_{fk-1}}{T} + a_{fk} = k_p a_k, \qquad (2.6)$$

where T is the sampling time of the estimation routine. The linear acceleration, as a discrete variable, is expressed as

$$a_{fk} = c_f a_k + c_{ff} a_{fk-1} \qquad (2.7)$$

where c_f and c_{ff} are constants obtained by

$$c_f = \frac{k_p T}{\tau + T}, \quad c_{ff} = \frac{\tau}{\tau + T}. \qquad (2.8)$$

For the implementation of the proposed estimation approach, the above equations are modified by introducing a scaling factor h to the bias term. This factor is determined by the designer of the estimation algorithm. The expression for the accelerometer output with the scaling factor is given below.

$$y_{Ak} = a_{fk} - g_{Ak} + hb_{Ak} + v_{Ak} \qquad (2.9)$$

Substituting (2.7) into (2.9) we obtain

$$y_{Ak} = c_f a_k + c_{ff} a_{fk-1} - g_{Ak} + hb_{Ak} + v_{Ak} \qquad (2.10)$$

11

2.2 Gyroscope Model

Gyroscopes are instruments to measure the angular motion rate along their axes. The gyroscope output signal can be written as the following sum of components [38]

$$y_{Gk} = \omega_k + b_{Gk} + v_{Gk} \qquad (2.11)$$

where y_G is the gyroscope output, v_G is the gyroscope noise and ω is the actual angular velocity. b_G is a bias term which evolves with

$$b_{Gk} = b_{Gk-1} + v_{bGk-1} \qquad (2.12)$$

2.3 Attitude representation

The attitude of the body frame may be described in a number of different ways [40]. Some of the most common ones are listed below:

2.3.1 Rotation matrices

A matrix in which the columns represent unit vectors in body axes projected along the reference axes is a rotation matrix. The element in the ith row and the jth column represents the cosine of the angle between the ith axis of the reference frame and the jth axis of the body frame. This representation is simple and it does not contain any singularities.

2.3.2 Euler angles

A transformation from one coordinate frame to another is defined by three successive rotations about the current principle axes. There are twelve Euler angles representations. An example is as follows: A rotation by angle ψ about reference z axis, followed by a rotation by angle θ about new y axis, and finally by a rotation by angle φ about the new x axis. The triplet (ψ, θ, φ) then describes the orientation of the body. This Euler angles representation can be termed as "z-y-x-Euler angles representation." This specific Euler angles representation is used in this thesis in addition to the unit quaternion representation reviewed below.

2.3.3 Axes angle representation

This type of attitude representation is based on the fact that a transformation from one coordinate frame to another can be done by a single rotation around a vector defined in a reference frame. The angle of the rotation θ and the unit vector in the direction of the rotation axis describe the orientation in this representation.

2.3.4 Quaternion for rigid body dynamics

The quaternion representation [41, 42] of a rigid body rotation is a four-dimensional vector representation of an arbitrary rotation around an axis [25]. The algebraic properties of quaternion distinguish them from other ordinary four-dimensional vectors. Some definitions and the computational principles are reviewed below.

2.3.4.1 Definitions

Definition 1. The quaternion vector consists of four elements vector. These elements are divided into two parts, scalar part $q_0 \in \mathbb{R}$ and vector part $\vec{n} \in \mathbb{R}^3$ as

$$q = q_0 + \vec{n} .$$ (2.13)

Equation (2.13) can be extended to write the quaternion in the form in (2.14) or simply as in (2.15)

$$q = q_0 + q_1 i + q_2 j + q_3 k$$ (2.14)

$$q = \begin{bmatrix} q_0 \\ q_1 \\ q_2 \\ q_3 \end{bmatrix}$$ (2.15)

Definition 2. Quaternion conjugate ($^{*}q$): Changing the sign of the rotational axis (the vector part) will form the quaternion conjugate, as described in (2.16),

$$^{*}q = q_0 - \vec{n} = q_0 - q_1 i - q_2 j - q_3 k$$ (2.16)

Definition 3. Quaternions Addition and subtraction ($q^1 \mp q^2$): both addition and subtraction are done in the same way. The scalar parts are added together or subtracted from each other. The vector parts are added component-wise as in (2.17)

$$q^1 \mp q^2 = \left(q_0^1 \mp q_0^2\right) + \left(q_1^1 \mp q_1^2\right)i + \left(q_2^1 \mp q_2^2\right)j + \left(q_3^1 \mp q_3^2\right)k$$ (2.17)

Definition 4. Quaternions multiplication ($q^1 q^2$): By referring to Definition 1 and Figure 2-1 , the product of two quaternions are

$$i^2=j^2=k^2=ijk=-1$$
$$ij=k, \ ji=-k$$
$$jk=i, \ kj=-i$$
$$ik=-j, \ ki=j$$
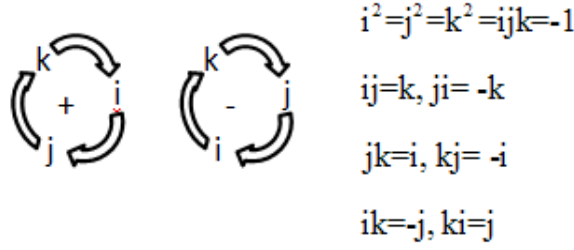
Figure 2-1: Quaternion unit vector multiplication

$$q^1 q^2 = \left(q_0^1 + q_1^1 i + q_2^1 j + q_3^1 k\right)\left(q_0^2 + q_1^2 i + q_2^2 j + q_3^2 k\right)$$

$$= \left(q_0^1 q_0^2 - q_1^1 q_1^2 - q_2^1 q_2^2 - q_3^1 q_3^2\right) +$$
$$\left(q_0^1 q_1^2 + q_1^1 q_0^2 + q_2^1 q_3^2 - q_3^1 q_2^2\right)i +$$
$$\left(q_0^1 q_2^2 - q_1^1 q_3^2 + q_2^1 q_0^2 + q_3^1 q_1^2\right)j +$$
$$\left(q_0^1 q_3^2 + q_1^1 q_2^2 - q_2^1 q_1^2 + q_3^1 q_0^2\right)k$$

(2.18)

(2.18) can be represented in the matrix form as

$$q^1 q^2 = \begin{bmatrix} q_0^1 & -q_1^1 & -q_2^1 & -q_3^1 \\ q_1^1 & q_0^1 & -q_3^1 & q_2^1 \\ q_2^1 & q_3^1 & q_0^1 & -q_1^1 \\ q_3^1 & -q_2^1 & q_1^1 & q_0^1 \end{bmatrix} \begin{bmatrix} q_0^2 \\ q_1^2 \\ q_2^2 \\ q_3^2 \end{bmatrix}$$

$$= \begin{bmatrix} q_0^2 & -q_1^2 & -q_2^2 & -q_3^2 \\ q_1^2 & q_0^2 & q_3^2 & -q_2^2 \\ q_2^2 & -q_3^2 & q_0^2 & q_1^2 \\ q_3^2 & q_2^2 & -q_1^2 & q_0^2 \end{bmatrix} \begin{bmatrix} q_0^1 \\ q_1^1 \\ q_2^1 \\ q_3^1 \end{bmatrix}$$

(2.19)

The quaternion multiplication is not commutative, i.e. $q^1 q^2 \neq q^2 q^1$.

From this point on, the quaternion multiplication will be assigned the symbol $\otimes$.

Definition 5. Quaternion Length: The quaternion length is the norm

$$\|q\| = \sqrt{q \otimes (*q)} = \sqrt{q_0^2 + q_1^2 + q_2^2 + q_3^2}$$

(2.20)

15

Definition 6. Quaternion inverse

$$q^{-1} = \frac{{}^{*}q}{\|q\|^2} \tag{2.21}$$

Definition 7. Augmented vector: A vector in $\mathbb{R}^3$ can be augmented with zero and transformed to $\mathbb{R}^4$ in a quaternion form. As an example the gravity would be in quaternion form as

$$g_q = \begin{bmatrix} 0 \\ g \end{bmatrix}$$

Theorem 1. [42] The rotation of vector g_q^1 around $\vec{n}$ by an angle α to produce a rotated vector g_q^2 is

$$g_q^2 = q \otimes g_q^1 \otimes q^{-1} \tag{2.22}$$

where q is a quaternion described as in (2.22) (2.15) . The inverse rotation is

$$g_q^1 = q^{-1} \otimes g_q^2 \otimes q \tag{2.23}$$

By arithmetic manipulation of (2.22), it can be shown that this rotation can be rewritten as

$$g^2 = R(q)g^1 \tag{2.24}$$

where *R(q)* is a rotation matrix described as

$$R(q) = \begin{bmatrix} q_0^2 + q_1^2 - q_2^2 - q_3^2 & 2(q_1 q_2 - q_0 q_3) & 2(q_1 q_3 + q_0 q_2) \\ 2(q_1 q_2 + q_0 q_3) & q_0^2 - q_1^2 + q_2^2 - q_3^2 & 2(q_2 q_3 - q_0 q_1) \\ 2(q_1 q_3 - q_0 q_2) & 2(q_2 q_3 + q_0 q_1) & q_0^2 - q_1^2 - q_2^2 + q_3^2 \end{bmatrix} \tag{2.25}$$

Theorem 2. [42] The quaternion derivative with respect to time can be expressed as

$$\dot{q} = 0.5U(\omega)q \tag{2.26}$$

where

16

$$U(\omega) = \begin{bmatrix} 0 & -\omega_x & -\omega_y & -\omega_z \\ \omega_x & 0 & \omega_z & -\omega_y \\ \omega_y & -\omega_z & 0 & \omega_x \\ \omega_z & \omega_y & -\omega_x & 0 \end{bmatrix} \tag{2.27}$$

and ω is the angular velocity vector as expressed in the body fixed frame. By rearranging equation (2.26), the form below can be obtained for $\dot{q}$.

$$\begin{aligned} \dot{q} &= 0.5U(\omega)q \\ &= 0.5 \begin{bmatrix} -\omega_x q_1 - \omega_y q_2 - \omega_z q_3 \\ \omega_x q_0 - \omega_y q_3 + \omega_z q_2 \\ \omega_x q_3 + \omega_y q_0 - \omega_z q_1 \\ -\omega_x q_2 + \omega_y q_1 - \omega_z q_0 \end{bmatrix} \\ &= 0.5\bar{U}(q)\omega \end{aligned} \tag{2.28}$$

where

$$\bar{U}(q) = \begin{bmatrix} -q_1 & -q_2 & -q_3 \\ q_0 & -q_3 & q_2 \\ q_3 & q_0 & -q_1 \\ -q_2 & q_1 & q_0 \end{bmatrix} \tag{2.29}$$

Definition 8. Quaternion to Euler angles conversion: Obtaining the Euler angles from the quaternion depends on the rotation order. The order considered here is x-y-z. In other words, first a roll rotation around the x-axis by an angle ϕ, then a pitch rotation about the current y-axis by an angle θ, and finally yaw rotation about the current z-axis by an angle ψ is carried out. The corresponding rotation matrix R is given by [43]

$$\begin{aligned} R &= R_{z,\psi} R_{y,\theta} R_{x,\phi} \\ &= \begin{bmatrix} c_\psi & -s_\psi & 0 \\ s_\psi & c_\psi & 0 \\ 0 & 0 & 1 \end{bmatrix} \begin{bmatrix} c_\theta & 0 & s_\theta \\ 0 & 1 & 0 \\ -s_\theta & 0 & c_\theta \end{bmatrix} \begin{bmatrix} 1 & 0 & 0 \\ 0 & c_\phi & -s_\phi \\ 0 & s_\phi & c_\phi \end{bmatrix} \\ &= \begin{bmatrix} c_\psi c_\theta & -s_\psi c_\phi + c_\psi s_\theta s_\phi & s_\psi s_\phi + c_\psi s_\theta c_\phi \\ s_\psi c_\theta & c_\psi c_\phi + s_\psi s_\theta s_\phi & -c_\psi s_\phi + s_\psi s_\theta c_\phi \\ -s_\theta & c_\theta s_\phi & c_\theta c_\phi \end{bmatrix} \end{aligned} \tag{2.30}$$

where the abbreviations c_ψ and s_ψ are used for $\cos(\psi)$ and $\sin(\psi)$, respectively. Comparing (2.25) with (2.30), it follows that the Euler angles can be expressed in terms of the quaternion parameters as

$$\psi = \tan^{-1}\left(\frac{2(q_1 q_2 + q_0 q_3)}{1 - 2(q_2^2 + q_3^2)}\right),$$
(2.31)

$$\phi = \tan^{-1}\left(\frac{2(q_2 q_3 + q_0 q_1)}{1 - 2(q_1^2 + q_2^2)}\right)$$
(2.32)

and

$$\theta = \sin^{-1}\left(-2(q_1 q_3 - q_0 q_2)\right)$$
(2.33)

2.3.4.2   Unit Quaternions

Quaternions with unit norm have an important role in representing rotations. Such a vector can be described as

$$q = \begin{bmatrix} \cos\left(\dfrac{\alpha}{2}\right) \\ \vec{n}\ \sin\left(\dfrac{\alpha}{2}\right) \end{bmatrix}$$
(2.34)

Here $\vec{n}$ represents the vector around which the rotation takes place, and α is the rotation angle (Figure 2-2).
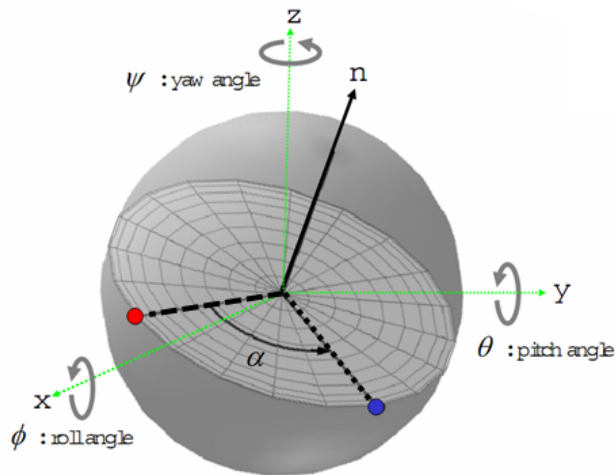
Figure 2-2: Quaternion representation of a rotation. In this example the dashed line is rotated to coincide with the dotted line.[25]

2.3.4.3 Advantages of the unit quaternion representation

The quaternion representation is attractive to be used because of the following advantages [44]:

- The angular discontinuities at $\pm\ \pi$ radians are avoided as well as the trigonometric singularities that can occur at $\pm\frac{\pi}{2}$ if compared with Euler angles
- They are more compact and faster than rotation matrices.
- Simple composition: The rotation is easily composed by multiplying the involved quaternions [41].

2.4 Kalman Filter

The Kalman filter is a statistically optimal estimator in the sense of minimizing the estimated error covariance. It is implemented as a programmed set of prediction and

19

correction equations that are called recursively to estimate the states of linear dynamic systems (Figure 2-3). The dynamic systems are perturbed by noise using noisy measurements that are linearly related to the state. Because of its simplicity and robustness nature, it has a great impact and used in many applications such as manufacturing systems, navigation systems [45, 46].

In the first part, i.e. in the prediction, a prior estimate based on the model at hand takes place, and then the correction part adjusts the predicted state vector using the measurements. In the following state space representation

$$x_k = F_{k-1}x_{k-1} + G_{k-1}u_{k-1} + w_{k-1}$$
$$y_k = C_k x_k + v_k$$

(2.35)

x is the state vector, u is the input vector and y is the output vector. F represents the state matrix, G is the input matrix and C is the output matrix. w and v are uncorrelated process and measurement zero mean Gaussian noise terms.

Then the Kalman filter algorithm is described by the following equations [45].

- Prediction:

$$\widehat{x}_k^- = F_{k-1}\widehat{x}_{k-1}^+ + G_{k-1}u_{k-1}$$
$$P_k^- = F_{k-1}P_{k-1}F_{k-1}^T + Q_{p,k-1}$$

(2.36)

- Correction

$$K_k = P_k^- C_k^T \left(C_k P_k^- C_k^T + Q_{o,k} \right)^{-1}$$
$$\widehat{x}_k^+ = \widehat{x}_k^- + K_k \left(z_k - C_k \widehat{x}_k^- \right)$$
$$P_k^+ = \left(I - K_k C_k \right) P_k^-$$

(2.37)

Prediction

1. Propagate the state

$$\hat{x}_k^- = F_{k-1}\hat{x}_{k-1}^+ + G_{k-1}u_{k-1}$$

2. Propagate the error covariance

$$P_k^- = F_{k-1}P_{k-1}F_{k-1}^T + Q_{p,k-1}$$

Initialization for x and P

Correction

1. Kalman filter gain

$$K_k = P_k^- C_k^T \left(C_k P_k^- C_k^T + Q_{o,k} \right)^{-1}$$

2. State update according to the current input

$$\hat{x}_k^+ = \hat{x}_k^- + K_k \left(z_k - C_k \hat{x}_k^- \right)$$

3. Covariance error update

$$P_k^+ = \left(I - K_k C_k \right) P_k^-$$
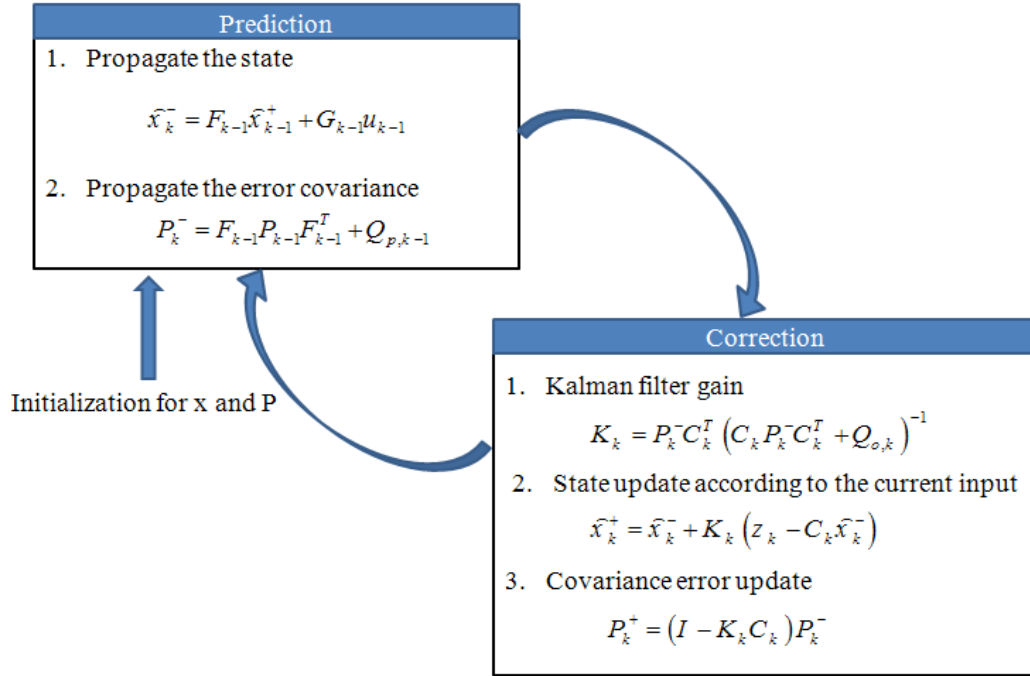
Figure 2-3: Kalman filter algorithm

In (2.36) and (2.37) the following notation is employed. $(.)^-$ and $(.)^+$ stand for the prior and posterior estimates, respectively. P is the estimation error covariance matrix and K is the Kalman gain. Q_p and Q_o stand for the process and measurement covariance matrices, respectively.

2.5   Extended Kalman Filter

It is a nonlinear version of Kalman filter. It uses a nonlinear state equation for prediction and linearizes the model around the current states for the correction stage. The nonlinear model is written as

$$x_k = f\left(x_{k-1}, u_{k-1}\right) + w_{k-1}$$
$$z_k = h\left(x_k\right) + v_k$$

(2.38)

21

where w and v are the process and observation zero mean Gaussian noises with covariance Q and R respectively. Then the prediction and update equations are as follows.

- Prediction

$$\hat{x}_{k|k-1} = f\left(\hat{x}_{k-1|k-1}, u_{k-1}\right)$$

$$P_{k|k-1} = F_{k-1} P_{k-1|k-1} F_{k-1}^{T} + Q_{k-1}$$

(2.39)

- Update

$$\tilde{y}_{k} = z_{k} - h\left(\hat{x}_{k|k-1}\right)$$

$$S_{k} = H_{k} P_{k|k-1} H_{k}^{T} + R_{k}$$

$$K_{k} = P_{k|k-1} H_{k}^{T} S_{k}^{-1}$$

$$\hat{x}_{k|k} = \hat{x}_{k|k-1} + K_{k} \tilde{y}_{k}$$

$$P_{k|k} = \left(I - K_{k} H_{k}\right) P_{k|k-1}$$

(2.40)

Here, the state and observation matrices are defined as

$$F_{k-1} = \left.\frac{\partial f}{\partial x}\right|_{\hat{x}_{k-1|k-1}, u_{k}}$$

$$H_{k} = \left.\frac{\partial h}{\partial x}\right|_{\hat{x}_{k|k-1}}$$

(2.41)

In these equations, $\hat{x}$ is the state vector, and u is the input. $\tilde{y}$ stands for the measurement residual. P is the estimation error covariance matrix and K is the Kalman gain.

3   GRAVITY VECTOR ESTIMATION

In this section, the general form of the output equation of the accelerometer in (2.9) is used for the estimation. A decomposition for the accelerometer signal is carried out to predict the additive terms in the accelerometer output to initialize the accelerometer Kalman filter. A z-y-x-Euler angles representation is employed to describe the orientation of the robotic platform (body). The Kalman filter corrected estimate of the gravity vector is used to calculate the x- and y- Euler angles. As mentioned in Chapter 1, the information contained in these angles is transformed into a quaternion vector to be used in the correction part of the gyroscope Extended Kalman filter explained in Chapter 4.

3.1   Acceleration Signal Decomposition

The accelerometer output in equation (2.10) (ignoring the noise) is

$$y_{Ak} = c_f a_k + c_{ff} a_{f\,k-1} - g_{Ak} + hb_{Ak} \qquad (3.1)$$

where a is the acceleration of the center of the body frame, as expressed in the body frame coordinates. We assume that the body frame axes coincide with the accelerometer measurement axes. $a_{f\,k-1}$ is updated each sample time to be the previous value of equation (2.7) taking into account the zero initial value.

Rewriting equation (3.1) in matrix form we obtain

$$y_A = \underbrace{\begin{bmatrix} c_f I_3 & -I_3 & h I_3 \end{bmatrix}}_{A} \begin{bmatrix} a \\ g_A \\ b_A \end{bmatrix} + c_{ff} a_{f\,k-1} \qquad . (3.2)$$

where I_n is the $n \times n$ identity matrix .

The acceleration and bias vector can then be computed as

$$\begin{bmatrix} a \\ g_A \\ b_A \end{bmatrix} = A^\dagger \left(y_A - c_{ff} a_{f\,k-1} \right) \qquad (3.3)$$

where $A^\dagger$ stands for the right pseudo inverse of a matrix A, obtained by

$$A^\dagger = A^T \left(A A^T \right)^{-1} \qquad (3.4)$$

In this way the prediction of the gravity in the body frame is done if (3.4) does exist. It does indeed exist since A is of full-rank. This computation is carried out only in the first estimation cycle, to initialize estimation.

After being calculated by (3.3), the values of the accelerometer signal terms are used in a Kalman filter as initial state estimates. This Kalman filter referred to as the "accelerometer Kalman filter" in this thesis.

3.2 Accelerometer Measurement State Space Model

The source for the acceleration a can be deliberate robot motion. It can originate from undesired falling or gliding motion too. In fact there are a large variety of scenarios in which the robotic platform accelerates and our estimation should be independent of these scenarios. Therefore the simplest possible acceleration model is assumed as the starting point in our modeling:

$$a_k = a_{k-1} + v_{a\,k-1} \qquad (3.5)$$

$$g_{Ak} = g_{Ak-1} + v_{g\,k-1} \qquad (3.6)$$

24

Here v_a and v_g are the linear and gravity acceleration zero mean Gaussian noises respectively. With these assumptions, the process model can be described as

$$x_k = \begin{bmatrix} a \\ g_A \\ b_A \end{bmatrix}_k = \begin{bmatrix} I_3 & 0 & 0 \\ 0 & I_3 & 0 \\ 0 & 0 & I_3 \end{bmatrix}_{k-1} \begin{bmatrix} a \\ g_A \\ b_A \end{bmatrix}_{k-1} + \begin{bmatrix} v_a & 0 & 0 \\ 0 & v_g & 0 \\ 0 & 0 & v_b \end{bmatrix}_{k-1} \tag{3.7}$$

In order to work on an output equation, (2.10) is repeated here for convenience:

$$y_{Ak} = c_f a_k + c_{ff} a_{f\,k-1} - g_{Ak} + hb_{Ak} + v_{Ak} \tag{3.8}$$

This equation can be put in the following form.

$$\underbrace{y_{Ak} - c_{ff} a_{f\,k-1}}_{\text{Meaured}} = \underbrace{c_f a_k - g_{Ak} + hb_{Ak} + v_{Ak}}_{z_k} \tag{3.9}$$

In this form, the left hand side terms can be identified as "measured" terms. y_{Ak} is literally measured since it is the accelerometer output signal. $c_{ff} a_{f\,k-1}$, on the other hand is not measured actually. However, it belongs to the previous cycle and is already computed before time index k. Therefore, we can treat the left hand side as a pseudo-measurement term. Note that all the terms on the right hand side of (3.9) are noise or scaled parts of the state vector in (3.7). Defining this left hand side as z_k, the following output equation can be written

$$z_k = \left(c_f a_k - g_{Ak} + hb_{Ak} + v_{Ak} \right) \tag{3.10}$$

which can be rearranged as

$$z_k = A \begin{bmatrix} a \\ g_A \\ b_A \end{bmatrix}_k + v_{Ak} \tag{3.11}$$

This completes the state space model of accelerometer based measurement used in this thesis.

3.3 Prediction

Ignoring the noise terms, the following version of (3.7) is employed for state prediction.

$$x_{k|k-1} = \begin{bmatrix} \hat{a} \\ \hat{g}_A \\ \hat{b}_A \end{bmatrix}_{k|k-1} = \begin{bmatrix} I_3 & 0 & 0 \\ 0 & I_3 & 0 \\ 0 & 0 & I_3 \end{bmatrix}_{k-1|k-1} \begin{bmatrix} \hat{a} \\ \hat{g}_A \\ \hat{b}_A \end{bmatrix}_{k-1|k-1} \tag{3.12}$$

The estimated output is then computed as

$$\hat{z}_{k|k-1} = A \begin{bmatrix} \hat{a} \\ \hat{g}_A \\ \hat{b}_A \end{bmatrix}_{k|k-1} . \tag{3.13}$$

3.4 Correction

The measurement residual is computed by the following equation.

$$\tilde{y}_k = \left(y_{Ak} - c_{ff} a_{f\,k-1} \right) - \hat{z}_{k|k-1} \tag{3.14}$$

The Kalman filter algorithm described in the previous chapter is then implemented by using the following settings for the filter matrices.

$$F_{k-1} = \begin{bmatrix} I_3 & 0 & 0 \\ 0 & I_3 & 0 \\ 0 & 0 & I_3 \end{bmatrix}, \; G_{k-1} = 0, \; C_k = A \tag{3.15}$$

The initial covariance matrices for the process and measurement noises are set randomly.

3.5 Euler Angle Computations

Calculating the x- and y-Euler angles is necessary for two main reasons. The first one is to use them in an orientation estimation mechanism based on the accelerometer signal only. The second one is to transform them into a unit quaternion representation to be used as the measured data in the Extended Kalman filter correction stage in the next chapter to estimate the orientation. The roll and pitch angles are calculated using

$$\theta = \sin^{-1}\left(\frac{g_{Ax}}{9.81}\right), \tag{3.16}$$

and

$$\phi = \sin^{-1}\left(\frac{g_{Ay}}{\cos(\theta) \times -9.81}\right) \tag{3.17}$$

3.6 Euler Angles to Unit Quaternion Representation

The accelerometer estimation for the roll and pitch angles operates in the low frequency ranges. Therefore, to overcome this limitation, its output data is fused with the gyroscope. Basically, since the output of the gyro based estimation is a unit quaternion, the estimated angles from the accelerometer Kalman filter are transformed into a unit quaternion representation too. However, to accomplish this transformation, the z-Euler angle is needed too. This angle is calculated from the estimated and non-corrected quaternion in (4.16) in the next chapter. In the first cycle however, this angle is assumed to be zero.

As mentioned in Chapter 2, with the z-y-x-Euler angles ψ, θ and ϕ about the current z, y and x=axes, respectively, the rotation matrix representation of the orientation is

$$R = R_{z,\psi} R_{y,\theta} R_{x,\phi} \tag{3.18}$$

27

and the corresponding quaternion can be computed as

$$q = \left(\cos(\psi/2) + k\,\sin(\psi/2)\right)\left(\cos(\theta/2) + j\,\sin(\theta/2)\right)\left(\cos(\phi/2) + i\,\sin(\phi/2)\right) \ . \ (3.19)$$

(3.19) yields the unit quaternion

$$q_A = \begin{bmatrix} q_{A0} \\ q_{A1} \\ q_{A2} \\ q_{A3} \end{bmatrix} = \begin{bmatrix} \cos(\phi/2)\cos(\theta/2)\cos(\psi/2) + \sin(\phi/2)\sin(\theta/2)\sin(\psi/2) \\ \sin(\phi/2)\cos(\theta/2)\cos(\psi/2) - \cos(\phi/2)\sin(\theta/2)\sin(\psi/2) \\ \cos(\phi/2)\sin(\theta/2)\cos(\psi/2) + \sin(\phi/2)\cos(\theta/2)\sin(\psi/2) \\ \cos(\phi/2)\cos(\theta/2)\sin(\psi/2) - \sin(\phi/2)\sin(\theta/2)\cos(\psi/2) \end{bmatrix} \qquad (3.20)$$

The notation "q_A" reads as the quaternion computed by the *A*ccelerometer based estimation method.

4   ORIENTATION ESTIMATION

The method proposed in this chapter uses the gyroscope angular rate signal to obtain a unit quaternion prediction which describes the orientation of the robotic platform. The estimation algorithm follows the guidelines of an Extended Kalman Filter.

A state space model of the angular rate measurement system is obtained firstly. The unit quaternion and the gyroscope bias are augmented to construct the state vector. A continuous-time quaternion dynamics equation is used as the starting point in modeling. This equation is discretized and combined with the gyroscope bias dynamics equation (2.12) to complete the state space model.

The resulting model, which is a nonlinear one, is used in the state prediction stage. The quaternion part of the predicted state vector is used as the predicted output. To serve as the measured output in the correction stage of the Extended Kalman Filter a second quaternion estimation is computed from the accelerometer measurements. This estimate is based on the gravity vector prediction presented in the previous chapter. The difference between the two quaternion estimates and the linearized versions of the state space equations are employed in the estimate correction stage.

Details of this estimation procedure, the quaternion initialization mechanism and measures for preserving the unity norm of the quaternion are presented below.

4.1 State Space Model of Gyroscope Signal Measurement

The derivation of the estimator starts with the expressions(2.26) and(2.27) for the quaternion dynamics. These equations are repeated below for convenience:

$$\dot{q} = \frac{1}{2}U(\omega)q \tag{4.1}$$

$$U(\omega) = \begin{bmatrix} 0 & -\omega_x & -\omega_y & -\omega_z \\ \omega_x & 0 & \omega_z & -\omega_y \\ \omega_y & -\omega_z & 0 & \omega_x \\ \omega_z & \omega_y & -\omega_x & 0 \end{bmatrix} \tag{4.2}$$

Here q is a unit quaternion which describes the orientation of the robotic platform (body) with respect to a world fixed reference frame. ω is the body angular velocity as expressed in the body coordinate frame. From (2.11), the vector ω can be written in terms of the gyroscope output signal y_G, gyroscope bias b_G and measurement noise v_G as

$$\omega = y_G - b_G - v_G \tag{4.3}$$

Hence, the quaternion dynamics in (4.1) can be expressed as

$$\dot{q} = \frac{1}{2}U(y_G - b_G - v_G)q \tag{4.4}$$

For a small sampling period T, this equation can be approximated by

$$\frac{q_k - q_{k-1}}{T} = \frac{1}{2}U(y_{Gk-1} - b_{Gk-1} - v_{Gk-1})q_{k-1}. \tag{4.5}$$

Here k stands for the sampling index. Rearranging(4.5) we obtain the following discrete time approximation of (4.4).

$$q_k = (I_{4\times4} + \frac{1}{2}TU(y_{Gk-1} - b_{Gk-1} - v_{Gk-1}))q_{k-1}. \tag{4.6}$$

The equation governing the dynamics of the gyroscope measurement bias was stated earlier in Chapter 2. This equation is repeated here too:

$$b_{Gk} = b_{Gk-1} + v_{bGk-1} \tag{4.7}$$

Defining the state vector x_k as

$$x_k \equiv \begin{bmatrix} q_k \\ b_{Gk} \end{bmatrix} \tag{4.8}$$

and the input u_k as y_{Gk}, the discrete-time dynamics equations for the quaternion q and the gyroscope measurement bias in (4.6) and (4.7), respectively, can be combined as

$$x_k \equiv \begin{bmatrix} q_k \\ b_{Gk} \end{bmatrix} = \begin{bmatrix} (I_{4\times4} + \frac{1}{2}TU(y_{Gk-1} - b_{Gk-1} - v_{Gk-1}))q_{k-1} \\ b_{Gk-1} + v_{bGk-1} \end{bmatrix} \tag{4.9}$$

From (4.2) and (4.9) we have:

$$x_k \equiv \begin{bmatrix} (I_{4\times4} + \frac{1}{2}TU(y_G - b_G))q_{k-1} \\ b_{Gk-1} \end{bmatrix} + \begin{bmatrix} \frac{1}{2}TU(-v_{Gk-1})q_{k-1} \\ v_{bGk-1} \end{bmatrix} \tag{4.10}$$

Defining the state matrix $f(x_{k-1}, u_{k-1})$ as

$$f(x_{k-1}, u_{k-1}) \equiv \begin{bmatrix} (I_{4\times4} + \frac{1}{2}TU(y_{Gk-1} - b_{Gk-1}))q_{k-1} \\ b_{Gk-1} \end{bmatrix} \tag{4.11}$$

and the process noise w_k as

$$w_{k-1} \equiv \begin{bmatrix} \frac{1}{2}TU(-v_{Gk-1})q_{k-1} \\ v_{bGk-1} \end{bmatrix} \tag{4.12}$$

(4.9) can be rewritten as

$$x_k = f(x_{k-1}, u_{k-1}) + w_{k-1} \tag{4.13}$$

Although the term $TU(-v_G)q_{k-1}$ in (4.12) is state dependent, this dependency is ignored as a simplification, and w_k is considered as an independent noise term. This simplification is justified by the fact that the components of the unit quaternion q_{k-1} are always constrained to have magnitudes less than or equal to one, making drastic changes in the noise effect impossible.

The output z_k of this state space system is chosen as q_k. This choice has a special reason: We would like to use the difference between the predicted output (the quaternion prediction generated by gyroscope data) with the measured output (the quaternion obtained from the accelerometer data) in the correction stage. With this choice, the computation of z_k can be carried out by a matrix multiplication as

$$z_k = H_G x_k + v_k \tag{4.14}$$

where

$$H_G \equiv \begin{bmatrix} I_{4 \times 4} & 0_{4 \times 3} \end{bmatrix} \tag{4.15}$$

In (4.15) $0_{4 \times 3}$ stands for a 4×3 matrix with zero entries. The notation H_G reads as "the output matrix H used in the Gyroscope based estimation." v_k is a measurement noise term.

4.2   Prediction

From (4.10) we obtain the following state prediction equation.

$$\hat{x}_{k|k-1} = f(\hat{x}_{k-1|k-1}, u_{k-1}) = \begin{bmatrix} (I_4 + \frac{1}{2} TU(y_{Gk-1} - \hat{b}_{Gk-1|k-1}))\hat{q}_{k-1|k-1} \\ \hat{b}_{Gk-1|k-1} \end{bmatrix} \tag{4.16}$$

The computation of the predicted output $\hat{z}_k$ is carried out by

$$\hat{z}_{k|k-1} = H_G \hat{x}_{k|k-1} \tag{4.17}$$

4.3 Correction

The matrix H_G in (4.14) can be used in the Extended Kalman Filter covariance and state update equations described in Chapter 2 as is. However, the expression in (4.16), for $f(\hat{x}_{k-1|k-1}, u_{k-1})$ is nonlinear and it has to be approximated by a Jacobian before it can be used in these equations. This Jacobian, here denoted by F_{Gk-1}, is computed as follows. First of all $f(\hat{x}_{k-1|k-1}, u_{k-1})$ is rewritten in a form more convenient for partial derivative computations with respect to the components of $\hat{b}_{Gk-1|k-1}$. Using the linearity of $U(\cdot)$ we have:

$$f(\hat{x}_{k-1|k-1}, u_{k-1}) = \begin{bmatrix} (I_4 + \frac{1}{2}TU(y_{Gk-1}) - \frac{1}{2}TU(\hat{b}_{Gk-1|k-1}))\hat{q}_{k-1|k-1} \\ \hat{b}_{Gk-1|k-1} \end{bmatrix} \quad (4.18)$$

Further, using the identity in (2.28) we can write

$$U(\hat{b}_{Gk-1|k-1})\hat{q}_{k-1|k-1} = \bar{U}(\hat{q}_{k-1|k-1})\hat{b}_{Gk-1|k-1} \quad (4.19)$$

to obtain

$$f(\hat{x}_{k-1|k-1}, u_{k-1}) = \begin{bmatrix} (I_4 + \frac{1}{2}TU(y_{Gk-1}))\hat{q}_{k-1|k-1} - \frac{1}{2}T\bar{U}(\hat{q}_{k-1|k-1})\hat{b}_{Gk-1|k-1} \\ \hat{b}_{Gk-1|k-1} \end{bmatrix} \quad (4.20)$$

Indeed, the form in (4.20) makes the partial derivative computations with respect to the components of $\hat{b}_{Gk-1|k-1}$ more straightforward. The matrix F_{Gk-1} is then computed as

$$F_{Gk-1} = \frac{\partial f(\hat{x}_{k-1|k-1}, u_{k-1})}{\partial \hat{x}_{k-1|k-1}} = \begin{bmatrix} (I_4 + \frac{1}{2}TU(y_{Gk-1} - \hat{b}_{Gk-1|k-1})) & -\frac{1}{2}T\bar{U}(\hat{q}_{k-1|k-1}) \\ 0_{3\times4} & I_{3\times3} \end{bmatrix} \quad (4.21)$$

Equipped with the matrices H_G and F_{Gk-1}, the correction is carried out by following the main structure of the Extended Kalman Filter described in Chapter 2. In this computation, in equations (2.39)-(2.40) the matrices H_k and F_{k-1} are replaced by

H_G and F_{Gk-1}, respectively. Also, $H_G \hat{x}_{k|k-1}$ replaces $h(\hat{x}_{k|k-1})$ and the quaternion estimate q_A based on the accelerometer readings is used in place of z_k. The initial process and measurement noise covariances are assigned randomly.

4.4   Initial State Estimation

In order to start the prediction cycle, (4.16) needs an initial state estimate which can be denoted by $\hat{x}_{0|0}$. $\hat{x}_{0|0}$ is composed of the initial quaternion and bias estimates:

$$\hat{x}_{0|0} = \begin{bmatrix} \hat{q}_{0|0} \\ \hat{b}_{G\,0|0} \end{bmatrix} \tag{4.22}$$

The initial gyroscope bias estimate $\hat{b}_{G0|0}$ is set to a zero vector. This choice is motivated by observations in our experiments: Estimate convergence to actual values was faster with small initial bias.

The quaternion estimate is initialized using the body frame gravity vector estimate g_{A0} obtained in the first computational cycle by the accelerometer based method described in the previous chapter. The value of the z-axis Euler angle ψ used in (3.20) is zero for the initial quaternion estimate $\hat{q}_{0|0}$.

4.5   Preserving the Unity Norm of the Quaternion Estimate

The estimation procedure presented in Sections 4.1-4.3 does not include a mechanism to preserve the unit norm of the quaternion. Therefore a numerical norm correction method is employed after the estimation in each computational cycle. The value $\|q\| = 1$ can be imposed on the estimated quaternion by introducing $(1 - \|q\|)q$ as a correction term. If the norm is greater or less than one, a portion of the quaternion will be subtracted from or added to the corrected quaternion according to

$$\hat{q}_{U\,k|k} = \hat{q}_{k|k} + \left(1 - \left\|\hat{q}_{k|k}\right\|\right)\hat{q}_{k|k} \tag{4.23}$$

where $\hat{q}_{k|k}$ is the last estimated quaternion, and $\hat{q}_{U\,k|k}$ is the norm corrected quaternion. $\hat{q}_{U\,k|k}$ replaces $\hat{q}_{k-1|k-1}$ in the next iteration of the prediction.

5   EXPERIMENTAL RESULTS

In this chapter, implementation results are presented with two orientation estimation techniques. One of them is the method presented in Chapter 3 the estimation with accelerometer data only. As in previous chapters, this method is referred to as "Accelerometer Kalman Filter" (AKF). The second method implemented is the one presented in Chapter 4: "Gyroscope Extended Kalman Filter" (GEKF). In order to test the proposed estimation algorithms, experiments are conducted on a 3D robotic platform. The next section introduces the test setup and experimental results follow.

5.1   Experimental 3D platform

An experimental platform is designed and built to test the algorithms. It is equipped with encoders and an IMU at the top of the platform.

5.1.1   The IMU

The IMU used for the measurement is the crossbow VG440 as in Figure 5-1. Its outputs are 3-axes acceleration and 3-axes angular velocity. The outputs are filtered using analog low-pass filters and then sampled and converted to digital data at a frequency of 1 kHz. The sensor data is filtered and down-sampled to 100Hz by the on board DSP using FIR filters [51]. Therefore, delay time in the output estimated results is expected.
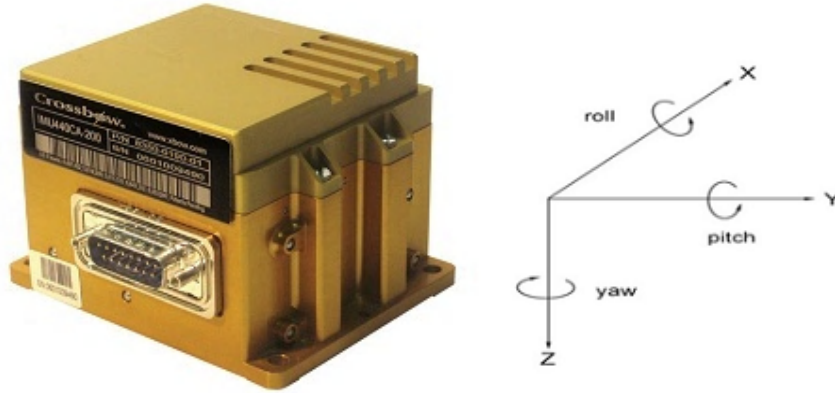
Figure 5-1: IMU Crossbow VG440 with its frame

5.1.2   3D Robotic Platform

A 3D manipulator (Figure 5-2) is designed at the Sabanci University Robotics Research Laboratory for the experiments. The links of the platform are machined and assembled at Sabanci University too. The orientation of the tool end can be computed exactly using the joint position measurements obtained from the three encoders attached to the motors. Orientation obtained from actual robot joint positions is used as a base for comparison in the evaluation of the performance of the estimation algorithms. The comparison is made over z-y-x-Euler angles. The robot joint angles are used in a forward kinematics scheme to obtain a rotation matrix representing the tool frame (sensor frame) orientation. Inverse kinematics is used then to compute the corresponding z-y-x-Euler angles of the tool frame. The output of the AKF algorithm is readily in the form of x- and y-Euler angles and the unit quaternion representation obtained from the GEKF is converted to z-y-x-Euler angles by using ((2.31)-(2.33)) in order to serve in the comparisons.
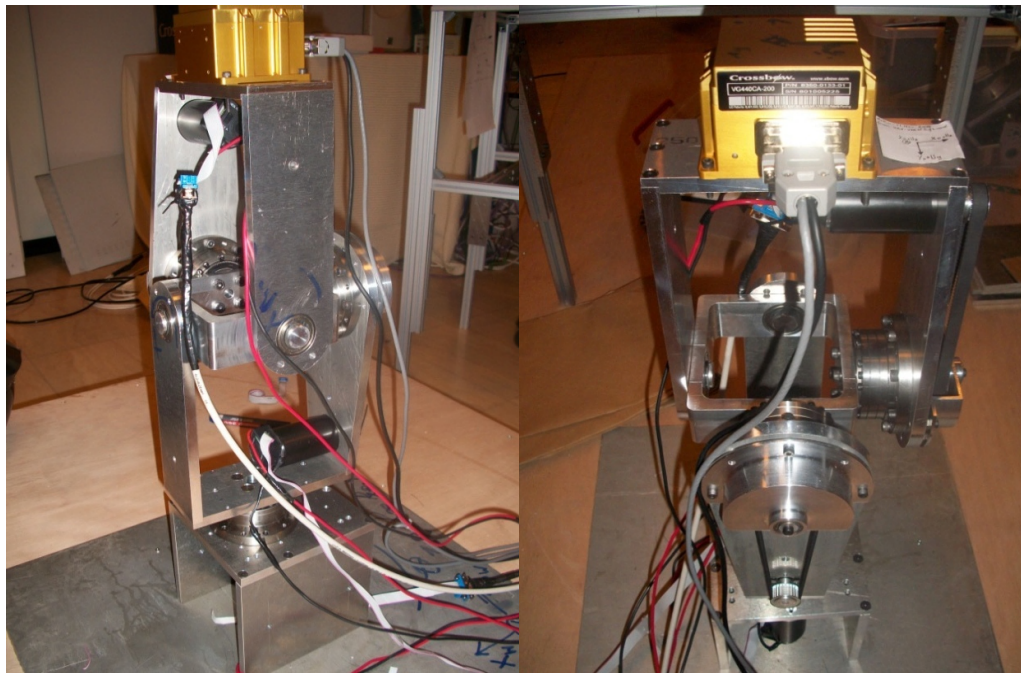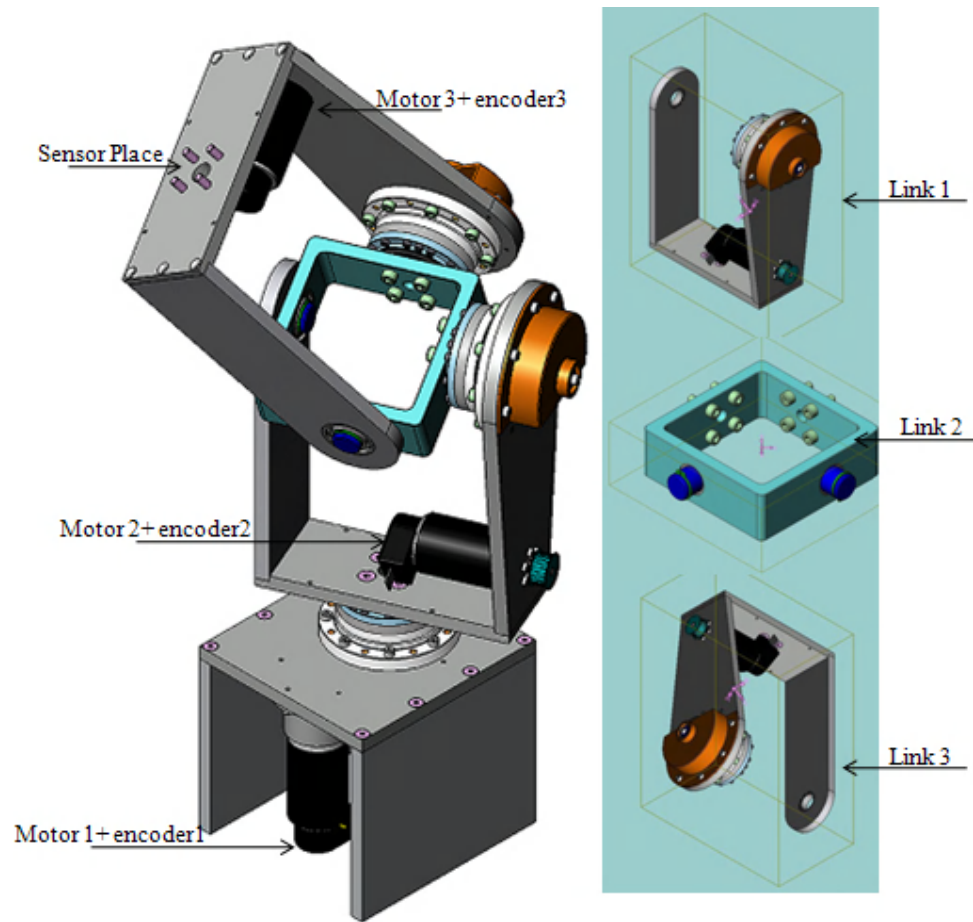
Figure 5-2: Experimental 3D Platform

An independent joint PID controller is employed for the position control of the manipulator (Figure 5-3). The controller parameters are listed in Table 5-1. A controller sampling time of 1 ms is used. Step, sinusoidal and superposition of step and sinusoidal position references can be generated for the robot joint over a graphical user interface.
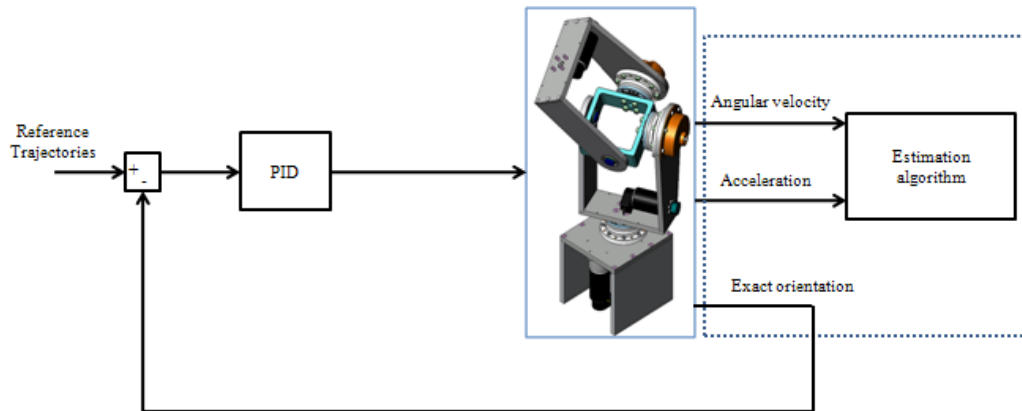

Figure 5-3: System control

Table 5-1: Controller Parameters

	Motor 1	Motor 2	Motor 3
K_p (proportional gain)	15	40	21
K_i (integral gain)	5	0.05	0.09
K_d (derivative gain)	4	7	2

5.2 Experimental Results

In this section, the predicted orientations using the proposed estimation algorithms are compared against the exact orientation (calculated using the motor encoder data). The employed estimation sampling time is 0.01 sec. With this sampling time, it is reasonable to expect that the estimation algorithms presented can be implemented in microcontroller based computing units, without overloading them, too.

5.2.1 Mode one: Step input

Figure 5-4 shows the estimation using both the sensor fusion algorithm (GEKF) and accelerometer Kalman filter (AKF) with exact orientation of the robot (RD) for the step input case. The estimation from both filters matches the exact value. The GEKF is smoother especially when sudden changes occur.
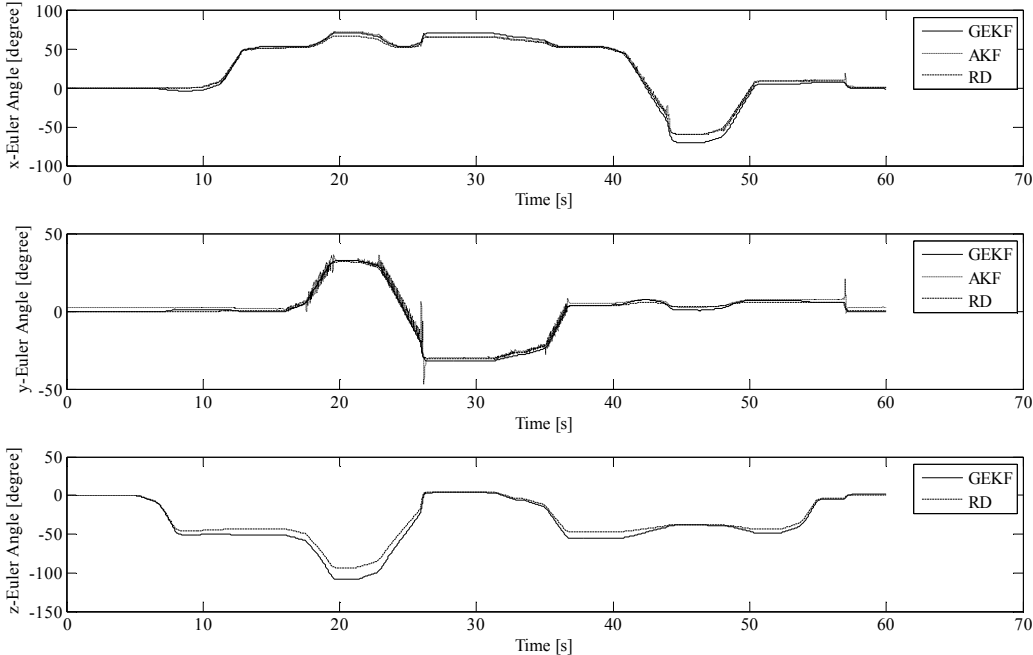

Figure 5-4: Step input for robot joint angles. GEKF: Estimation using the sensor fusion in the extended Kalman filter, AKF: Estimation using the accelerometer Kalman filter only, and RD: Robot data.

5.2.2 Mode Two: Sinusoidal Input

Figure 5-5 and its zoomed version, Figure 5-6, indicate the success of the sensor fusion with the GEKF estimation algorithm with sinusoidal motion. The AKF estimation based on the accelerometer only is no longer reliable. Although the z-Euler angle estimation solely relies on the gyroscope measurements, its estimation is reliable

most of the time. The zero point of the z-Euler angle estimation is the initial angle of the platform at the beginning of the estimation
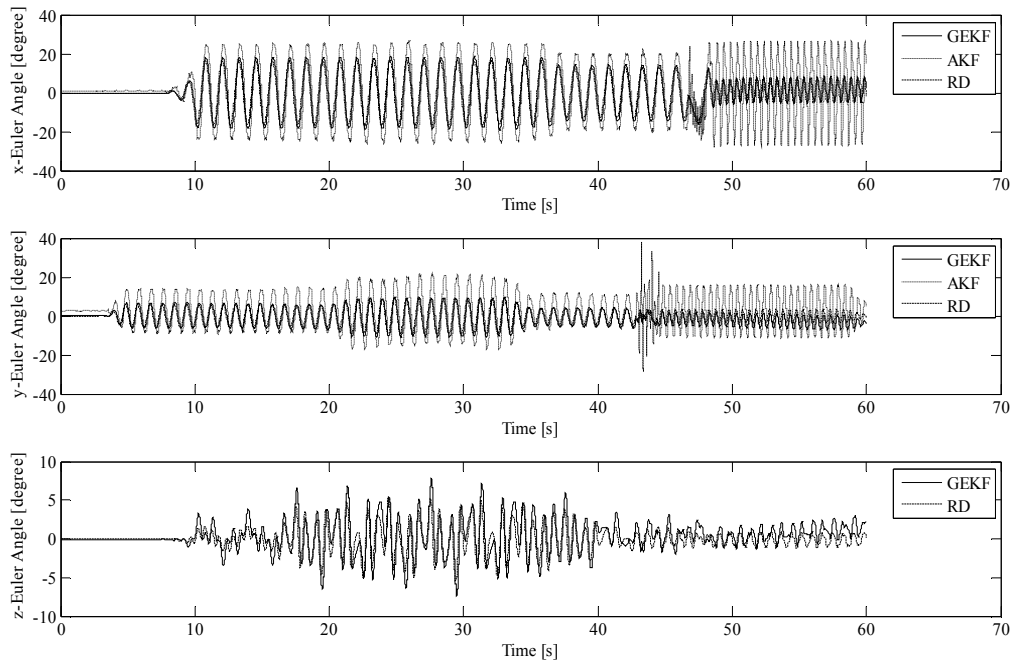

Figure 5-5: Sinusoidal input for robot joint angles. GEKF: Estimation using the sensor fusion in the extended Kalman filter, AKF: Estimation using the accelerometer Kalman filter only, and RD: Robot data.
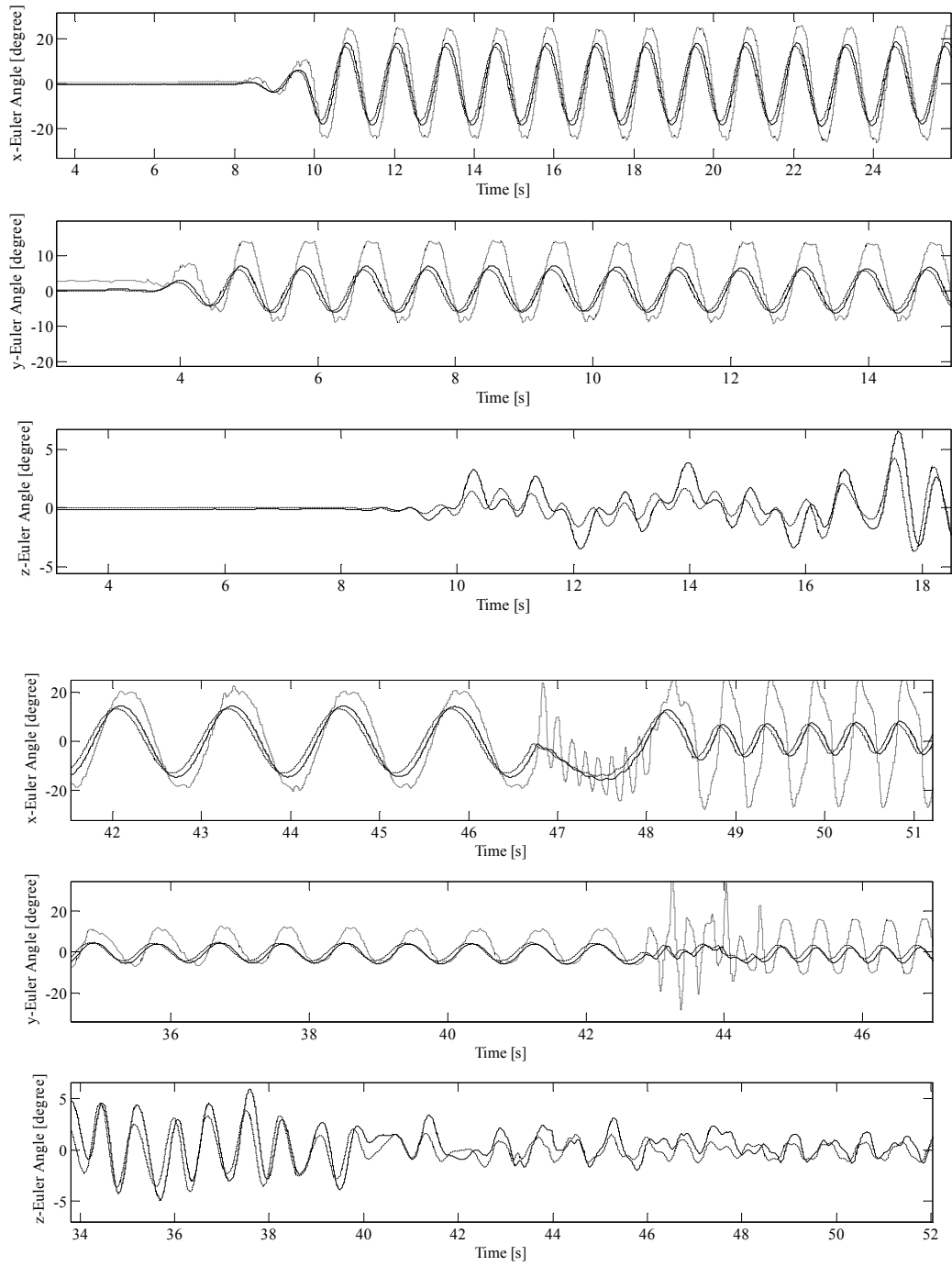
Figure 5-6: A zoom into Figure 5-5

5.2.3 Mode Three: Step and Sinusoidal Input

In this mode a step references are applied to the platform for each of the three joints and after that a sinusoidal angle is applied too with variable amplitude and frequency. As it is clear from Figure 5-7 and its zoomed versions (Figure 5-8 and Figure 5-9), the GEKF algorithm estimates the orientation of the platform accurately. In the beginning of the estimation, the z-Euler angle is estimated with a considerably large error. However, the algorithm corrected this error as shown after the 20th second. The AKF estimation of an angle is sensitive to the other angles motion. This is apparent from the signals between the 13th and the 17th seconds where the actual x- angle is constant while the actual y-angle is sinusoidal: The AKF generated x-angle estimate is not constant in this period.
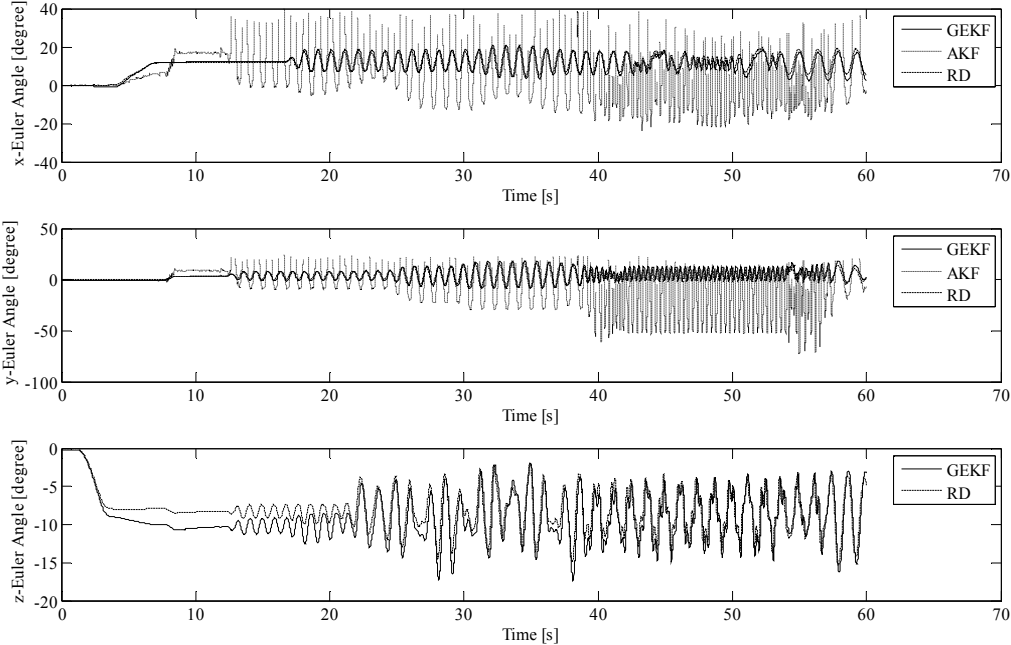

Figure 5-7: Step and sinusoidal joint position references. GEKF: Estimation using the sensor fusion in the extended Kalman filter, AKF: Estimation using the accelerometer Kalman filter only, and RD: Robot data.
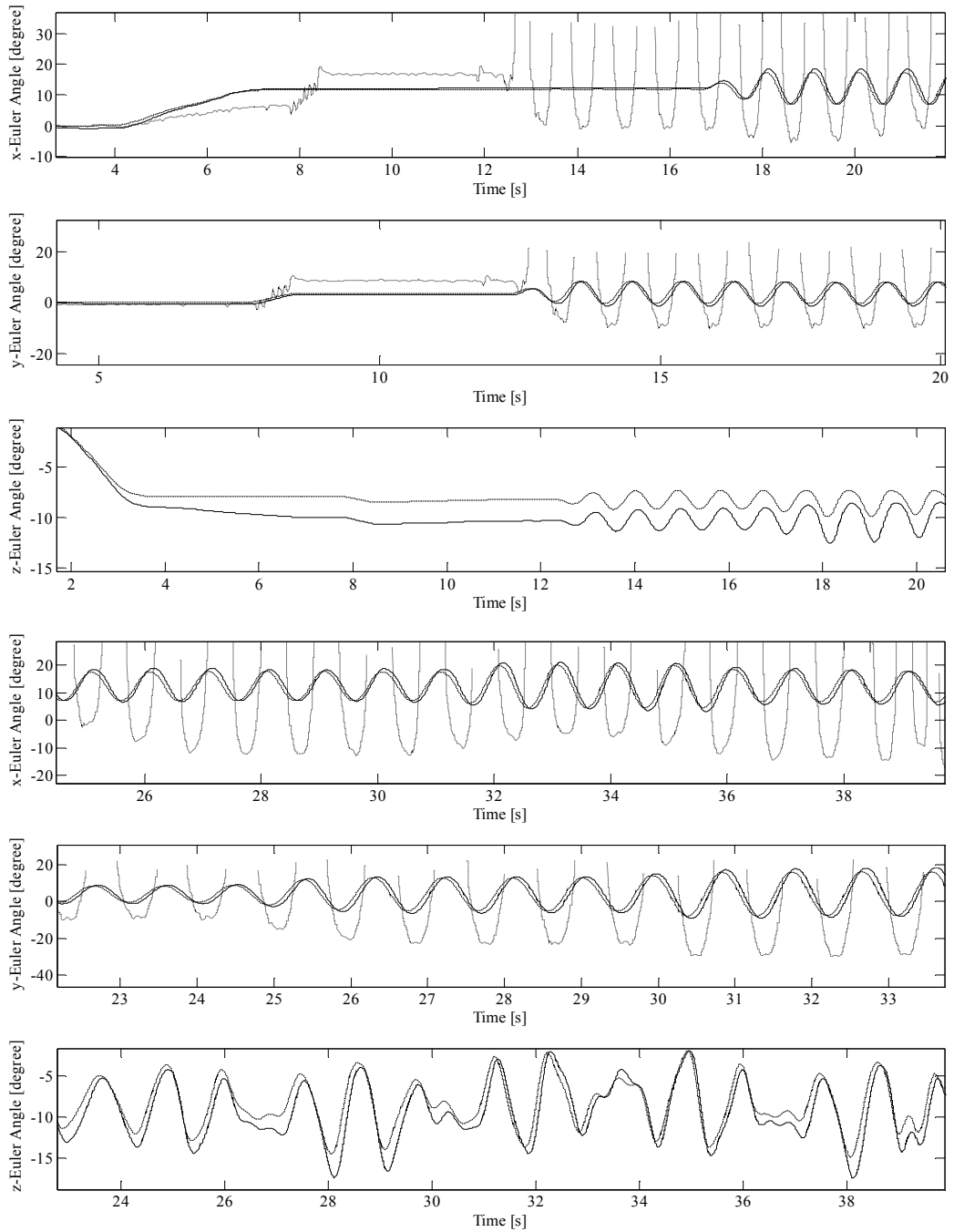
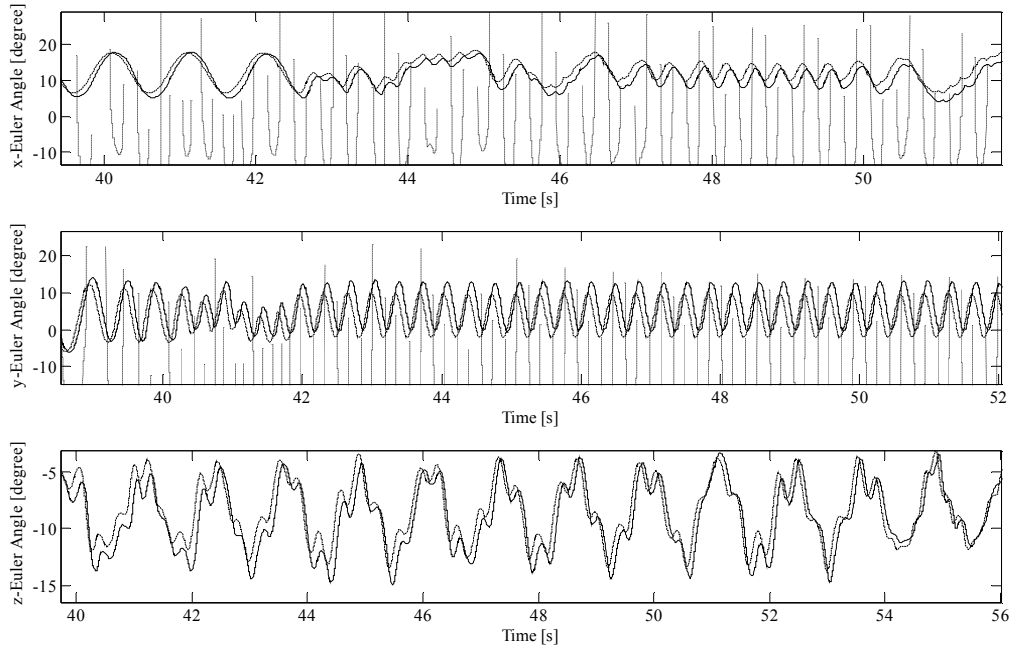Figure 5-8: A zoomed into Figure 5-7.

Figure 5-9: Another zoomed into Figure 5-7

5.2.4 A note on the drifts

Our longer duration experiments indicate that the estimates drift after around two minutes with the estimators proposed in this thesis. A tuning algorithm for the EKF feedback is needed in order to balance the bias estimate as in [51].

5.3 Results comparing with previous work

An EKF is implemented in [34] with sampling frequency 1 kHz based on inclinometer and gyroscope as explained before. As in our study, this work compares the estimated angles with angles computed from robot joint encoder data too. The results are close to each other in low frequency motion. [34] presents estimates with two Hz motion frequency as high frequency results, while in this thesis the experiments are conducted at more than three Hz. Also, in this thesis, the angular motion ranges are larger than the ones in [34] which reports a motion range of $\pm\ 30^{o}$.

6 CONCLUSION AND FUTURE WORK

In this thesis, an accelerometer signal decomposition is carried out and the gravity vector is estimated using an Accelerometer Kalman filter (AKF). x- and y-Euler angles are calculated using the estimated gravity vector and then transformed into quaternion representation. A second estimator, a full orientation estimation algorithm termed Gyroscope Extended Kalman Filter (GEKF) is designed and implemented too. This estimator fuses the estimated quaternion from the accelerometer and the estimated quaternion for the gyroscope readings. As a result, the z-y-x-Euler angles are estimated.

An experimental robotic platform was built and equipped with encoders. The encoder outputs are used in order to calculate the exact actual z-y-x-Euler angles. These actual angles are considered as references with which the estimated orientations are compared.

The estimated z-y-x-Euler angles calculated in the experiments using the GEKF algorithm match their reference counterparts accurately for a wide range of angular motion and frequencies. The algorithm runs smoothly. The experiments indicate that proposed GEKF is a robust and reliable orientation estimation scheme.

7   REFERENCES

[1] **P.G. Savage**. Strapdown inertial navigation integration algorithm design. Part 2: Velocity and position algorithms, Journal of Guidance, Control, and Dynamics 2 1 (2) (1998) 208–221.

[2] **V.K. Varadan, e t al**.. High sensitive and wide dynamic range navigation microsystem on a single chip. in: Proceedings of SPIE – The International Society for Optical Engineering, Melbourne, Australia, 2000, pp. 134–140.

[3] **Tatsuya Harada, Taketoshi Mori, Tomomasa Sato.** Development of a tiny orientation estimation device to operate under motion and magnetic disturbance. The International Journal of Robotics Research. 2007, Vol. 26, 6 pp.547-559.

[4]   **M.J. Caruso**, Applications of magnetic sensors for low cost compass systems, in: IEEE Position Location and Navigation Symposium, San Diego, 2000, pp. 177–184.

[5]   **Demoz Gebre-Egziabher, Roger C. Hayward, J . David Powell.**   Design of multi-sensor attitude determination systems. IEEE Transaction on Aerospace and Electronic System, 40 (2) (2004) 627–649.]

[6] **D. Gebre-Egziabber, G.H. Elkaim, J.D. Powell, B.W. Parkinson**. Gyro-free quaternion-based attitude determination system suitable for implementation using low cost sensors. in: IEEE PLANS, Position Location and Navigation Symposium, San Diego, 2000, pp. 185–192.

[7]   **D. Gebre-Egziabber, R.C. Hayward, J.D. Powell**. A low cost GPS/Inertial attitude heading reference system (AHRS) for general aviation applications. in: IEEE PLANS, Position Location and Navigation Symposium, Palm Springs, 1998, pp. 518–525.

[8] **Najib Metni, Jean-Michel Pflimlin, Tarek Hamel, Philippe Soueres.** Attitude and gyro bias estimation for a VTOL UAV. Control Engineering Practice. 2006, Vol. 14, pp.1511 – 1520.

[9] **Baerveldt, A.-J. Klang, R.** A low-cost and low-weight attitude estimation system for an autonomous helicopter. IEEE International Conference on Intelligent Engineering Systems, INES '97. Proceedings. 15-17 Sep 1997, pp.391-395.

[10] **A. Tayebi, S. McGilvray, A. Roberts and M. Moallem.** Attitude estimation and stabilization of a rigid body using low-cost sensors. Proceedings of the 46th IEEE Conference on Decision and Control. Dec. 12-14, 2007, New Orleans, LA, USA.

[11] **Kalman, R.E.** A new approach to linear filtering and prediction problems. Journal of Basic Engineering. 1960, 82:35–45.

[12] **Paul R. MacNeilage, Narayan Ganesan, and Dora E. Angelaki.** Computational Approaches to Spatial Orientation: From Transfer Functions to Dynamic Bayesian Inference. J Neurophysiol. 2008, Vols. 100: 2981–2996.

[13] **Rong Zhu, Dong Sun, Zhaoying Zhou, Dingqu Wang.** A linear fusion algorithm for attitude determination using low cost MEMS-based sensors. Measurement , 2007, Vol. 40. pp.322–328.

[14] **Xiaoping Yun, Mariano Lizarraga, Eric R. Bachmann! and Robert B. McGhee.** An Improved Quaternion-Based Kalman Filter for Real-Time Tracking Rigid Body Orientation. Proceedings of the 2003 IEEE/RSJ Inll. Conference on Intelligent Robots and Systems. October 2003, Las Vegas. Nevada.

[15] **João Luís Marins, Xiaoping Yun, Eric R. Bachmann, Robert B. McGhee, and Michael J. Zyda.** An Extended Kalman Filter for Quaternion-Based Orientation Estimation Using MARG Sensors. Maui, Hawaii, USA : Proceedings of the 2001 IEEE/RSJ International Conference on Intelligent Robots and Systems, Oct. 29 - Nov. 03, 2001.

[16] **M.D. Shuster and S.D. Oh**. Three-Axis Attitude Determination from Vector Observations. Journal of Guidance and Control, Vol. 4, No. 1, pp. 70-77, January-February 1981.

[17] **F. Landis Markley and Daniele Mortari**. Quaternion Attitude Estimation Using Vector Observations. The Journal of the Astronautical Sciences, Vol. 48, No. 2-3, pp. 359-380, 2000.

[18] **Xiaoping Yun, Conrado Aparicio, Eric R. Bachmann, and Robert B. McGhee.** Implementation and Experimental Results of a Quaternion-Based Kalman Filter for Human Body Motion Tracking. Proceedings of the 2005 IEEE International Conference on Robotics and Automation Barcelona, Spain, April 2005

[19] Robert B. McGhee. The Factored Quaternion Algorithm for Orientation Estimation from Measured Earth Gravity and Magnetic Field. Technical Memorandum, MOVES Institute, Naval Postgraduate School, Monterey, CA, June 2004. http://www.users.muohio.edu/bachmaer/Papers/Factored%20Q uaternion.pdf

[20] **Henrik Rehbinder, Xiaoming Hu.** Drift-free attitude estimation for accelerated rigid bodies. Automatica. 2004, Vol. 40, pp.653–659.

[21] **Sabatini, A. M.** Quaternion-based strap-down integration method for applications of inertial sensing to gait analysis. Medical & Biological Engineering & Computing. 2005, Vol. 43.

[22] **J. Favre, B.M. Jolles, O. Siegrist and K. Aminian.** Quaternion-based fusion of gyroscopes and accelerometers to improve 3D angle measurement. Electronics Letters 25th May 2006 Vol. 42 No. 11.

[23] **D. CHOUKROU N, I. Y. BAR-ITZHACK, Y. OSHMAN .** Novel Quaternion Kalman Filter. IEEE Transactions on Aerospace and Electronics systems. Vol. 42, No. 1 January 2006.

[24] **Manoranjan Majji, Daniele Mortari.** Quaternion Constrianed Kalman filter . Advances in the Astronautical Sciences, 2008.

[25] **BACHMANN, E. R.** Inertial and magnetic tracking of limb segment orientation for inserting humans in synthetic environments. s.l. : PhD thesis, Naval Postgraduate School, Monterrey, CA, USA , 2000.

[26] **H.J. Luinge, P.H. Veltink.** Measuring orientayion of human body segments using miniature gyroscopes and accelerometers. Medical & Biological Engineering and Computing. 2005, Vol. 43.

[27] **Eric Foxlin**. Inertial Head-Tracker Sensor Fusion by a Complimentary Separate-Bias Kalman Filter. vrais, pp.185, 1996 Virtual Reality Annual International Symposium (VRAIS 96), 1996

[28] **Necsulescu, Rahim Jassemi-Zargani and Dan.** Extended Kalman Filter-Based Sensor Fusion for Operational Space Control of a Robot Arm. IEEE Transactions on Instrumentation and Measurment. December 2002, vol 51,6.

[29] **Lefierts,E.J.,Markley,F.L.,andShuster,M.D**. Kalman Filtering for Spacecraft Attitude Estimation. Journal of Guidance, Control, and Dynamics, Vol.5,No.5,Sept.-Oct.1982,pp.417{429.

[30] **João Luís Marins, Xiaoping Yun, Eric R. Bachmann, Robert B. McGhee, and Michael J. Zyda.** An Extended Kalman Filter for Quaternion-Based Orientation Estimation Using MARG Sensors. Proceedings of the 2001 IEEE/RSJ International Conference on Intelligent Robots and Systems. Oct. 29 - Nov. 03, 2001, Vols. pp. 2003-2011, Maui, Hawaii, USA.

[31] **Farrell,J.L.** . Attitude Determination by Kalman Filter. Automatica, Vol.6, No 5, 1970, pp. 419-430.

[32] **Yilun Luo, Chi Chiu Tsang, Guanglie Zhang, Zhuxin Dong, Guangyi Shi,.** An Attitude Compensation Technique for a MEMS Motion Sensor Based Digital Writing Instrument. Proceedings of 2006 IEEE International Conference on Nano/Micro Engineered and Molecular Systems. 2006.

[33] **Rambabu Kandepu, Bjarne Foss, Lars Imsland.** Applying the unscented Kalman filter for nonlinear state estimation. Journal of Process Control. 2008, Vol. 18, 753–768.

[34] **Henrik Rehbinder , Xiaoming Hu.** Nonlinear Pitch and Roll Estimation for walking Robots. Proceedings of the 2000 IEEE International Conference on Robotics & Automation, San Francisco, CA April 2000.

[35] **Markley, F. L..** Attitude Error Representations for Kalman Filtering. Journal of Guidance, Control, and Dynamics, Vol. 63, No. 2, 2003, pp. 311–317.

[36] **Särkkä, Simo.** On Unscented Kalman Filtering for State Estimation of Continuous-Time Nonlinear Systems. Septemper 2007, Vol. 52, 9.

[37] **Crassidis, J. L. and Markley, F. L..** Unscented Filtering for Spacecraft Attitude Estimation. Journal of Guidance, Control, and Dynamics, Vol. 26, No. 4, 2003, pp. 536–542.

[38]. **Roetenberg, Daniel.** Inertial and magnetic sensing of human motion. s.l. : University of Twente, 2006.

[39] **Veltink, Henk J. Luinge and Peter H.** Inclination measurement of human movement using a 3-D accelerometer With autocalibration. IEEE Transaction on Nueral Systems and Rehabilitation Engineering. 2004, Vol. 12, 1.

[40] **Wimmer, Christian.** Position Measurement in Inertial Systems. [Online] April 2006. www14.informatik.tu-muenchen.de/konferenzen/.../5/.../Wimmer.pdf.

[41] **Dam, Erik B., Koch, Martin, Lillholm, Martin.** Quaternions, Interpolation and Animation. Technical Report DIKU-TR-98/5, Department of Computer Science, University of Copenhagen, Denmark, July, 1998, pp. 93, 7

[42] **Simo Sarkka.** Notes on Quaternions. Technical Report. Centre of Excellence in Computational Complex Systems Research, Helsinki University of Technology, June 28, 2007.

[43] **Mark W. Spong, M. Vidyasagar,** Robot Dynamics and Control, Wiley-Interscience, 1989

[44] **Merwe, Rudolph van der.** Sigma-Point K alman Filters for Probabilistic Inference in Dynamic State-Space Models. 2004.

[45] **Mohinder S. Grewal, Angus P. Andrews.** Kalman filtering: theory and practice using MATLAB. s.l. : Wiley-Interscience, 2001.

[46] **Simon, Dan.** Optimal State Estimation . s.l. : Wiley-Interscience, 2006.

[47] **Greg Welch, Gary Bishop.** An Introduction to the Kalman Filter. [Online] University of North Carolina at Chapel Hill, 2001. http://www.cs.unc.edu/~tracker/media/pdf/SIGGRAPH2001_CoursePack_08.pdf.

[48**] C.F. Kao, T.L. Chen**. Design and analysis of an orientation estimation system using coplanar gyro-free inertial measurement unit and magnetic sensors. Sensors and Actuators A 144 (2008) 251–262

[49] **Ronald Schoenberg**. Optimization with the Quasi-Newton Method. Aptech Systems, Inc. Maple Valley, WA,2001.

[50] **John P. Bentley.** Principles of Measurement Systems, Prentis Hall. 4th edition 2005.

[51]. 440 Series Inertial Systems, Crossbow Technology, 2007. [Online]. http://www.xbow.com/Products/Product_pdf_files/Inertial_pdf/VG440_Datasheet.pdf